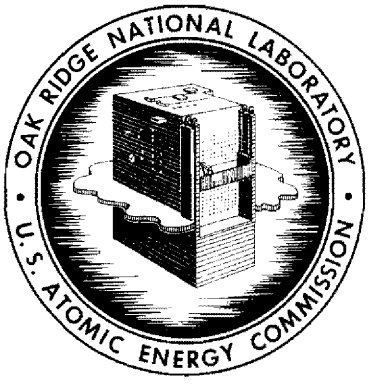

OAK RIDGE NATIONAL LABORATORY

operated by

UNION CARBIDE CORPORATION

for the

U.S. ATOMIC ENERGY COMMISSION

UNION CARBIDE

ORNL-TM-411

CORROSION OF NICKEL-BASE SPECIMENS EXPOSED IN THE VOLATILITY PILOT PLANT MARK III FLUORINATOR

T. M. Kegley, Jr.
A. P. Litman

ORNL-TM-411
Copy 2/

Contract No. W-7405-eng-26

METALS AND CERAMICS DIVISION

CORROSION OF NICKEL-BASE SPECIMENS EXPOSED IN THE VOLATILITY PILOT PLANT MARK III FLUORINATOR

T. M. Kegley, Jr., and A. P. Litman

DATE ISSUED

JAN 4 1963

OAK RIDGE NATIONAL LABORATORY
Oak Ridge, Tennessee
operated by
UNION CARBIDE CORPORATION
for the
U. S. ATOMIC ENERGY COMMISSION

CONTENTS

CORROSION OF NICKEL-BASE SPECIMENS EXPOSED IN THE VOLATILITY PILOT PLANT MARK III FLUORINATOR

T. M. Kegley, Jr., and A. P. Litman

INTRODUCTION

For several years the Volatility Pilot Plant has demonstrated the feasibility of processing zirconium-base fuels using fluoride volatility techniques. In an INOR-8 hydrofluorination vessel, rejected fully enriched zirconium-uranium alloy or dummy Zircaloy-2 fuel elements are dissolved at 500–600°C in NaF-LiF-ZrF_4 salts using an excess of anhydrous HF gas. Zirconium and uranium metal are converted to soluble tetrafluorides which subsequently are transferred, along with the fluoride bath, to a fluorination vessel. In the fluorinator, which is constructed of L nickel and operated at 500°C, elemental fluorine converts UF_4 to UF_6 product which is decontaminated and collected in cold traps. Figure 1 shows a simplified flowsheet of the volatility process.

Severe corrosion of the L nickel fluorinator occurs during processing. Three fluorinators have been used to date in the pilot plant, and all three have sustained a maximum corrosion attack of approximately 1 mil/hr, based on the fluorine exposure times.[1,2] Efforts to reduce the corrosive attack on fluorination vessels have included minimizing the operating temperature, careful exclusion of sulfur-containing compounds, and the search for a more resistant construction material. Accordingly, in the first two pilot plant fluorinators, Mark I and II, corrosion tests were performed using many potential container materials, mostly nickel-base alloys.[3]

---

[1]A. P. Litman and A. E. Goldman, Corrosion Associated with Fluorination in the Oak Ridge National Laboratory Fluoride Volatility Process, ORNL-2832, p 25 (June 5, 1961).

[2]A. P. Litman, Corrosion of Volatility Pilot Plant Mark I INOR-8 Hydrofluorinator and Mark III L Nickel Fluorinator After Fourteen Dissolution Runs, ORNL-3253, pp 1, 30 (Feb. 9, 1962).

[3]A. P. Litman and A. E. Goldman, op. cit., pp 108–23.

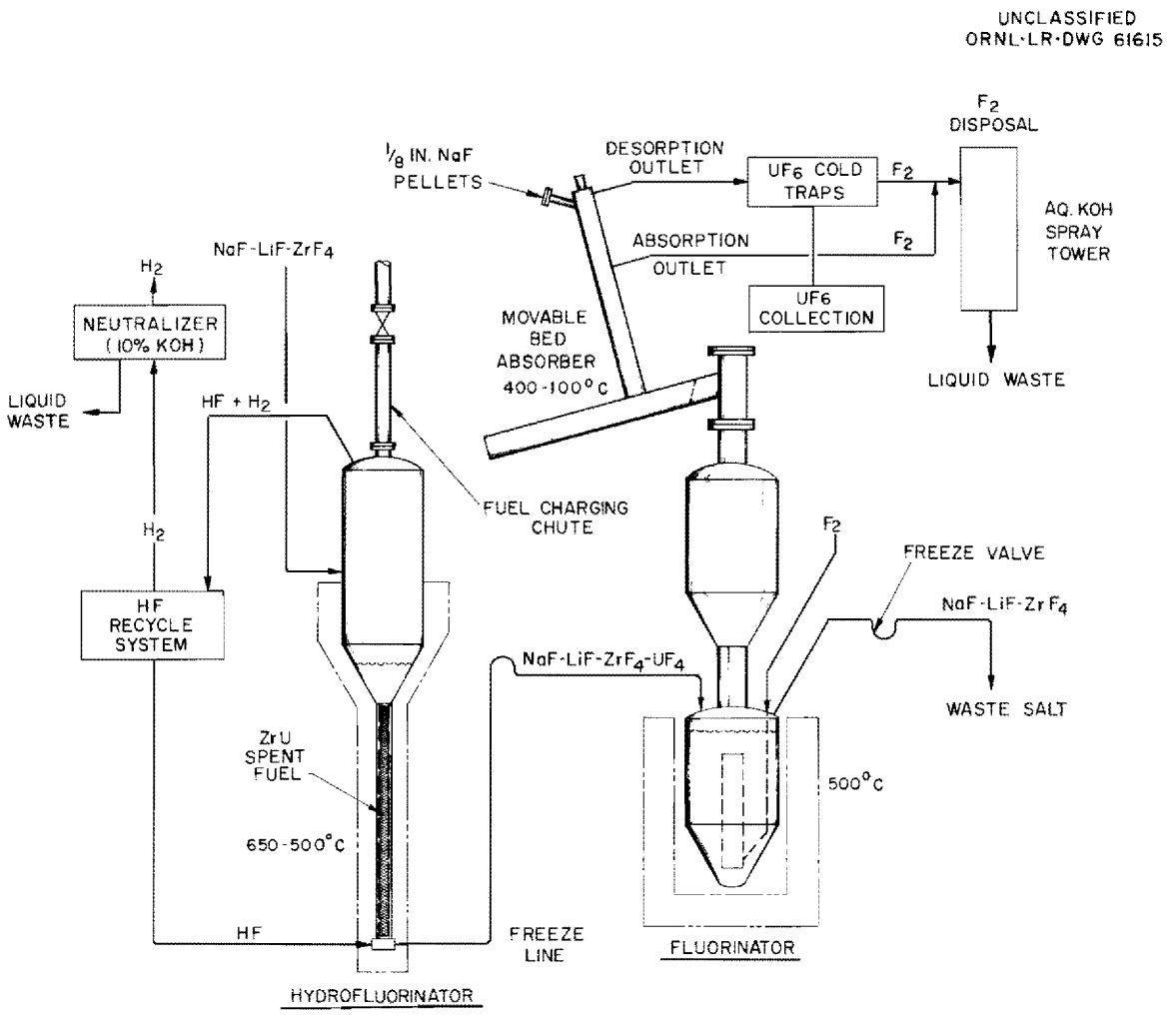

Fig. 1. Simplified Flowsheet — ORNL Fluoride Volatility Process.

Those nickel binaries containing iron, cobalt, or manganese showed improved corrosion resistance over L nickel and were thus selected for additional testing in the current Mark III fluorinator.

To date, 24 specimens have been exposed in the Mark III fluorinator. This report covers the 12 specimens comprising Groups I and II. Groups III and IV will be discussed in a separate report. In addition, specimens have been placed in the fluorinator for exposure during current runs where irradiated submarine fuel elements are being processed.

EXPERIMENTAL PROCEDURE

Specimen Description

Descriptions of the Group I and II test specimens, their location, and chemical compositions are shown in Tables 1 and 2. Control specimens containing the materials used in the construction of the fluorinator were included in both groups. The control specimens consisted of 3-in. lengths of $\frac{1}{4}$-in.-diam L nickel rod joined together with $\frac{1}{4}$-in. deposits of INCO-61 weld metal. The control specimen from Group I and one of the controls from Group II were fluorine conditioned for 3.2 hr at 600–645°C before testing to ascertain the effect of conditioning on corrosion.

The high-purity, vacuum-melted nickel specimen was obtained by remelting NiVac P nickel. Subsequently, the high-purity nickel was cast into a 1-in.-diam bar, cold swaged and cold drawn down to an 0.250-in. rod, and annealed at 1500°F.

The other binary alloys used in these tests were melted from virgin stock and cast into 1-in.-diam bars, cold swaged and cold drawn down to 0.250-in. rods. Subsequently they were annealed at 1650°F and placed in test.

Test Method

The specimen rods were located in nozzles attached to the lower chamber of the Mark III fluorination vessel, as shown in Fig. 2. Each rod was held in place by a fitting which gripped a tube prewelded to the end of the rod (see Fig. 3). Figure 4 shows a polar view of the fluorination chamber and the plan layout of the corrosion nozzles.

Table 1. Test Specimens Exposed in the Volatility Pilot Plant Mark III Nickel Fluorinator

Specimen No.	Nozzle Location	Description[a]
		Group I
51	O	L nickel, 3-in. lengths, joined by INCO-61 weld metal[b]
32	L	98 Ni–2 Mn
39	P	High-purity, vacuum-melted nickel
24R	R	95 Ni–5 Fe
27	M	90 Ni–10 Fe
29	N	80 Ni–20 Fe
		Group II
52	P	L nickel, 3-in. lengths, joined by INCO-61 weld metal[b]
55	N	L nickel, 3-in. lengths, joined by INCO-61 weld metal[c]
17	O	95 Ni–5 Co
21	R	90 Ni–10 Co
1R	M	99 Ni–1 Al
5	L	97 Ni–3 Al

[a] All rods approximately 0.250 in. diam × 36 in. long.

[b] Control specimen – fluorine conditioned for 5.3 hr at 560–670°C.

[c] Control specimen – not conditioned.

Table 2. Chemical Analyses of Test Specimens

Material	Weight Percent								(ppm)
	Ni	Mn	Fe	Co	Al	Si	Ti	C	S
98 Ni–2 Mn	97.00	2.18						0.057	40
95 Ni–5 Fe	95		4.9					0.019	< 10
90 Ni–10 Fe	88		11.8					0.016	< 10
80 Ni–20 Fe	79.6		20.1					0.017	< 10
95 Ni–5 Co	94.6			5.9				0.020	< 10
90 Ni–10 Co	90.0			9.4				0.026	20
99 Ni–1 Al					2.3			0.042	< 10
97 Ni–3 Al	96.4				3.0			0.027	< 10
INCO-61 weld metal deposit	96+	0.26	0.35		1.3	0.36	1.44	0.027	30
NiVac P high-purity Ni[a]		< 0.002	0.03	0.09	0.005			0.007	
L nickel[b]	99.0[c] min	0.35	0.40			0.35		0.02	100 max

[a] Trace amounts of Cr, Ca, Cu, Mg, and O_2.

[b] Nominal analysis.

[c] Including cobalt.

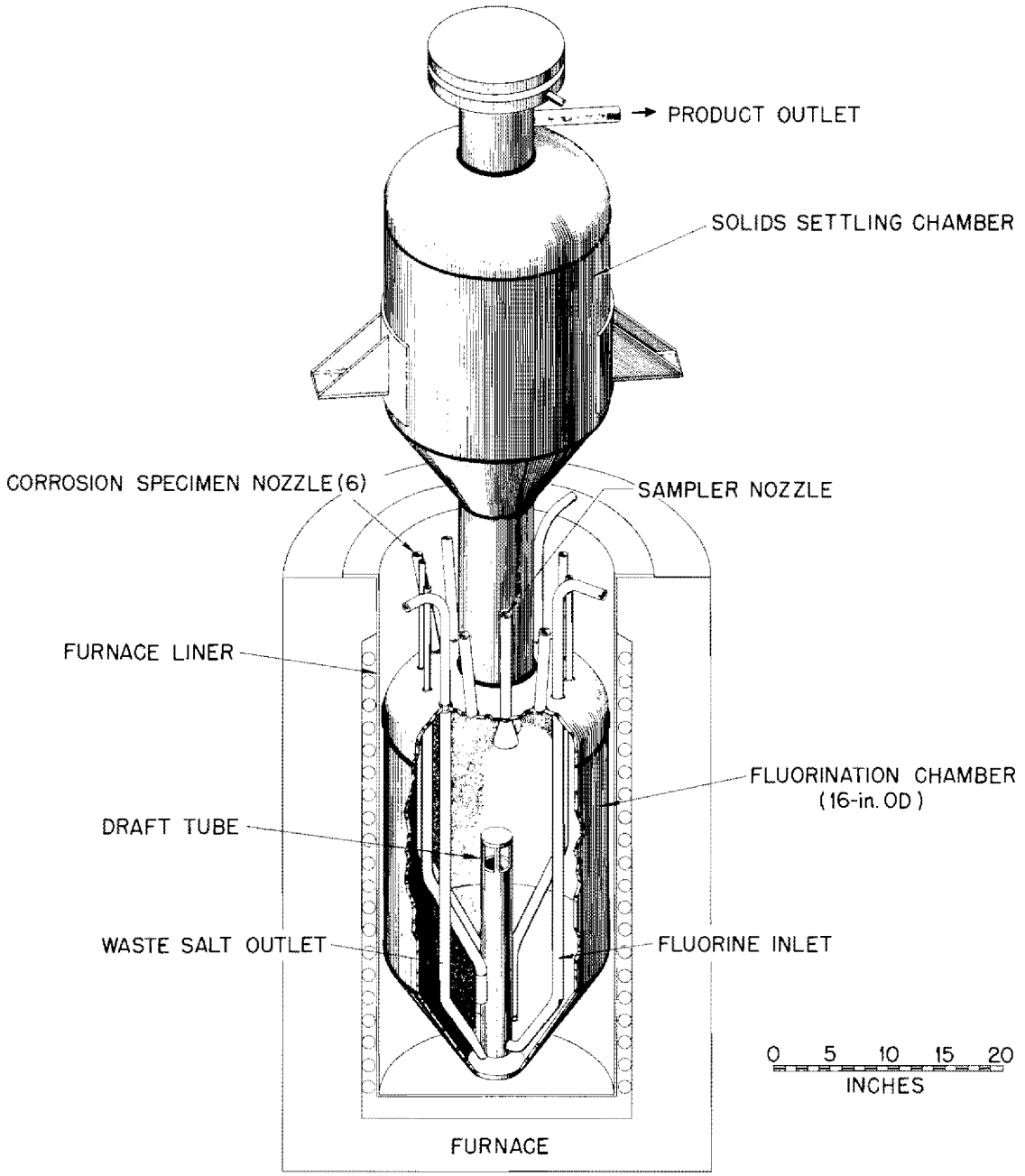

Fig. 2. Mark III Volatility Pilot Plant Fluorinator Vessel Showing Corrosion Specimen Nozzles.

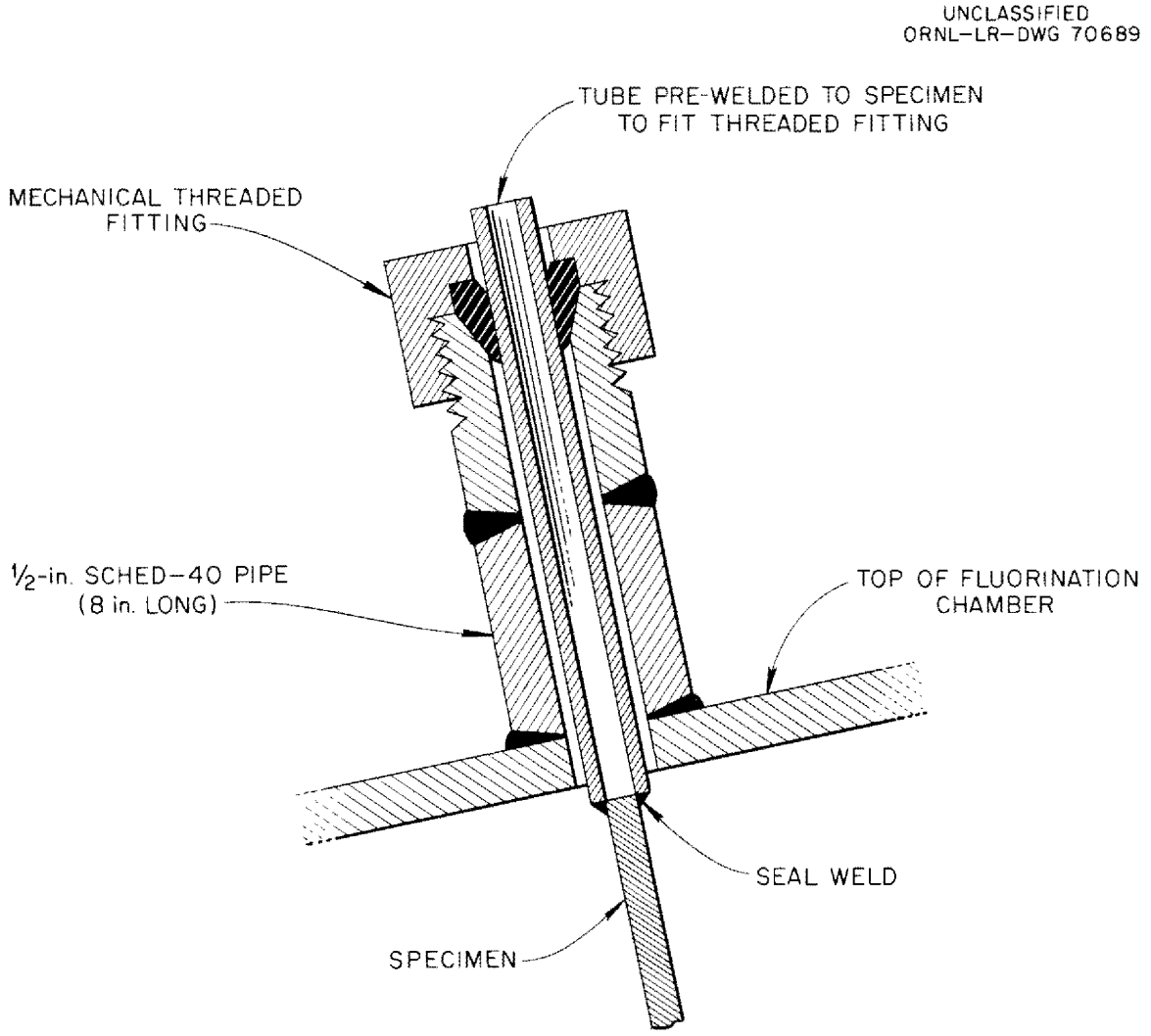

Fig. 3. Method for Holding Specimen Rods in Fluorinator Vessel.

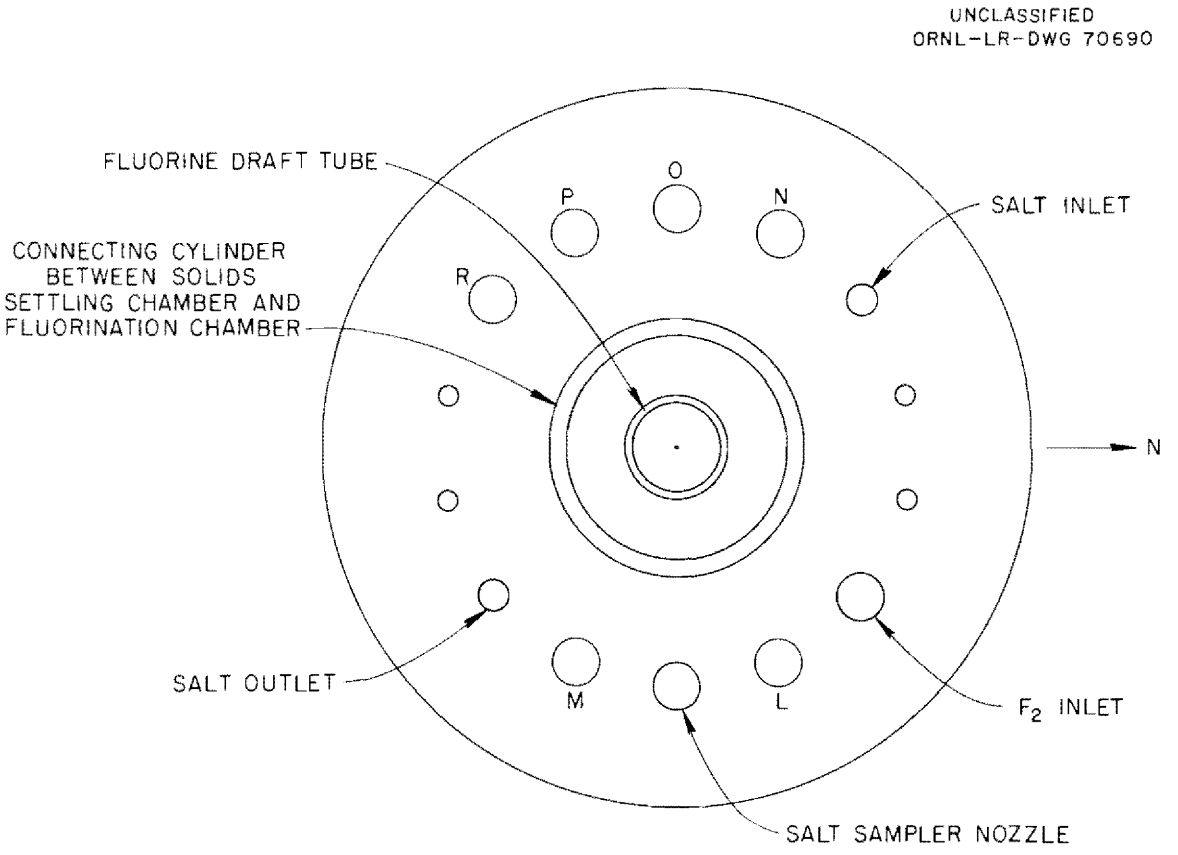

Fig. 4. Polar View of the Top of the Fluorination Chamber Showing Location of Corrosion Specimen Nozzles.

Test Conditions

The Group I corrosion specimens were exposed during Volatility Pilot Plant runs T-1 through T-7, while the Group II specimens were exposed in runs TU-1 through TU-5. Test conditions for these runs are summarized in Table 3. The T runs were made without uranium in the system, while the TU runs were conducted with 0.3 wt % U in the starting fuel element.

Table 3. Process Conditions for Groups I and II Corrosion Specimens

	Group I[a]	Group II
Volatility Pilot Plant Runs	T-1 through T-7	TU-1 through TU-5
Thermal cycles, room temperature to operating temperature	7	5
Salt composition, mole %	$LiF-NaF-ZrF_4$ (~ 30–27–43)	$LiF-NaF-ZrF_4$ (~ 29–29–42) + 0.3 wt % U
Molten salt exposure		
Time	367 hr	205.5 hr
Temperature	485–605°C	490–575°C
Fluorine exposure[b]		
Time	12.0 hr	10.5 hr
Temperature	535–570°C	500–515°C
Fluorine input	5760 liters	5385 liters
UF_6 exposure	None	256 liters

[a] L nickel and INCO-61 weld metal specimen 51 was fluorine conditioned for 5.3 hr at 600°C (before exposure to Group I process conditions).

[b] Molten salt was also present during fluorine exposure.

RESULTS

Visual Examination

Visual examination of the Group I specimens disclosed fluoride salts had preferentially adhered to the specimens in the vapor and salt-vapor interface regions. Figure 5 shows the Group I specimens after cleaning with an ammonium oxalate solution. Surface roughening was apparent in all the specimens, but no gross localized metal losses were evident.

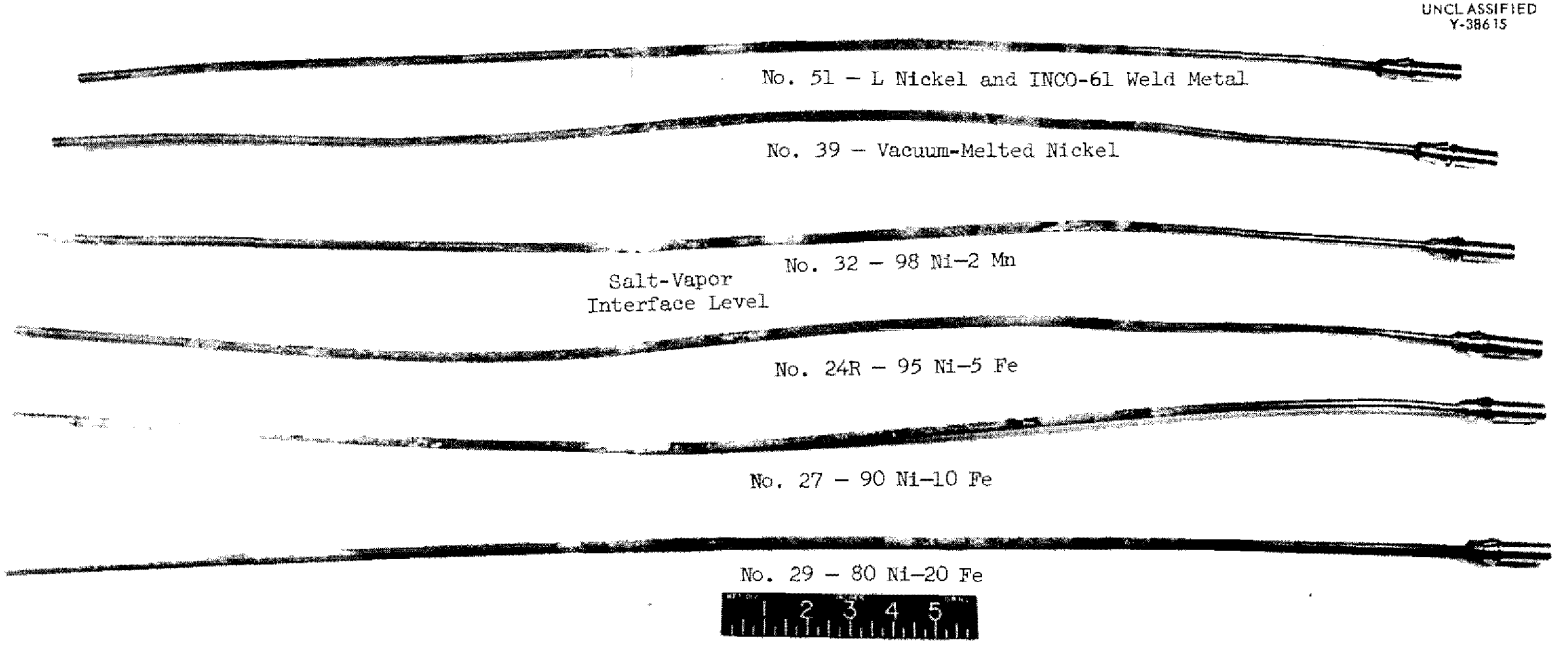

Fig. 5. Group I Corrosion Specimens from Mark III Fluorinator. Reduced 25%.

Examination of the Group II specimens showed fluoride salts had preferentially adhered to specimens in the lower vapor region. Some loosely adherent deposits were also noted in the interface region. Figure 6 shows the Group II specimens after an ammonium oxalate wash.

Dimensional Changes

Bulk metal losses from the specimens were determined from micrometer measurements taken in the vapor, vapor-salt interface, and salt-exposure regions. Table 4 details the results. The Group II specimens generally showed losses several times greater than the Group I specimens.

Metallographic Examination

Transverse and longitudinal sections taken from the vapor, interface, and salt regions of the corrosion specimens were examined using optical microscopy. Photomicrographs of most of these sections are included in the Appendix. Metallographic examination revealed that corrosion had resulted in the production of one or more of the following: (1) surface films, (2) surface attack, (3) intergranular attack, and (4) grain-boundary modifications.

Surface Films

Two types of surface films were observed — a gray nonmetallic and a bright semimetallic film. Usually the films were intermittent in coverage rather than continuous. Figure 7 illustrates the types of films found. Details regarding the surface films found on the specimens are summarized in Tables 5 and 6. Except for the Group I specimens showing a propensity for formation of bright films in the salt-exposed region, no particular pattern associating film formation with region of exposure of specimen composition was obvious.

Samples of the two types of surface films were obtained from an L nickel specimen using a microchisel[4] and submitted for x-ray diffraction analyses. A quantitative analysis could not be obtained, but the results,

---

[4]G. L. Kehl, H. Steinmetz, and W. J. McGonnagle, Metallurgia 55(329), 151 (1957).

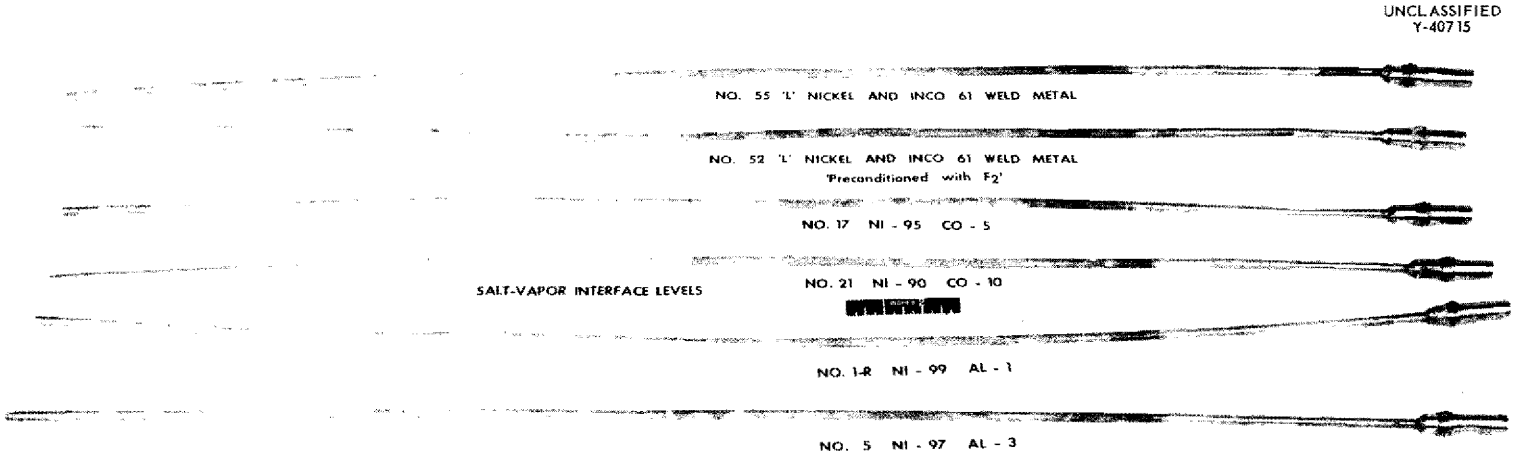

Fig. 6. Group II Corrosion Specimens from Mark III Fluorinator. Reduced 22%.

Table 4. Bulk Metal Losses for Groups I and II Corrosion Specimens

Specimen No.	Composition	Vapor Salt					
		Vapor Region		Interface Region		Salt Region	
		Max	Av	Max	Av	Max	Av
		Group I					
51[a]	L nickel	1.4	0.9	2.0	1.7	2.2	1.5
	INCO-61 weld metal	2.6	1.4	2.2	1.9	2.3	2.0
39	High-purity nickel	2.0	0.9	3.1	1.7	1.4	0.8
32	98 wt % Ni–2 wt % Mn	2.0	1.4	1.9	1.7	1.7	1.5
24R	95 wt % Ni–5 wt % Fe	1.7	0.9	1.4	1.3	2.1	1.7
27	90 wt % Ni–10 wt % Fe	1.9	1.1	1.8	1.5	1.7	1.4
29	80 wt % Ni–20 wt % Fe	2.9	1.4	1.4	1.0	1.9	1.6
		Group II					
52[a]	L nickel	2.9	1.75	9.1	8.4	7.1	5.9
	INCO-61 weld metal	5.4	4.8	12.1	12.0	13.4	12.4
55[b]	L nickel	2.7	2.4	11.4	8.9	7.1	6.3
	INCO-61 weld metal	4.0	1.9	13.5	11.95	7.3	7.1
17	95 wt % Ni–5 wt % Co	no change		13.4	10.5	11.9	9.2
21	90 wt % Ni–10 wt % Co	4.1	1.1	16.3	14.1	13.0	8.1
1R	99 wt % Ni–1 wt % Al	2.3	1.2	11.5	10.6	7.8	6.3
5	97 wt % Ni–3 wt % Al	3.5	1.6	17.2	12.3	8.3	7.4

[a]Control specimen fluorine conditioned 5.3 hr at 560–670°C.

[b]Control specimen not conditioned.

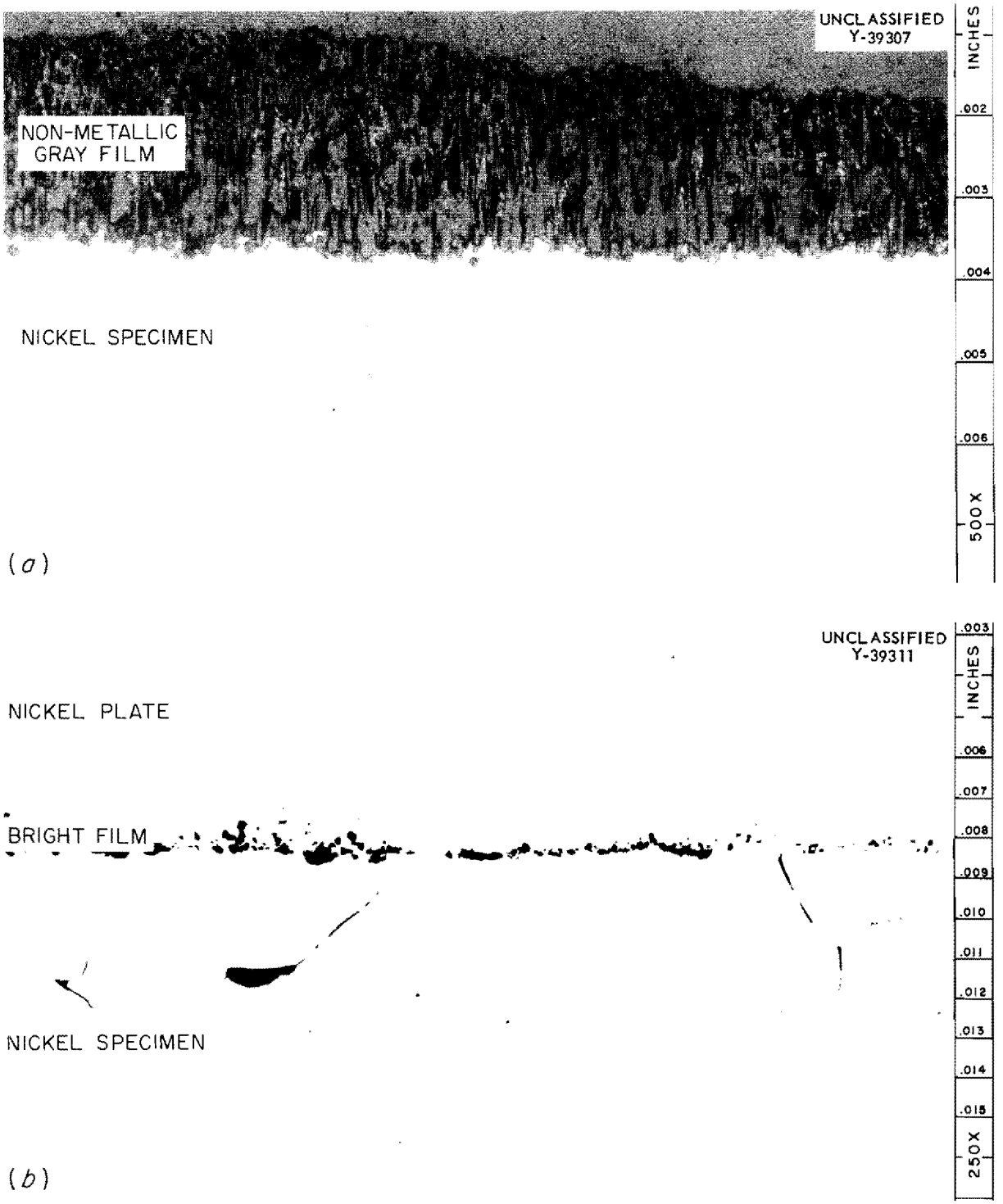

Fig. 7. Surface Films Found on Nickel Corrosion Specimens Exposed in Volatility Pilot Plant Mark III Fluorinator. (a) Gray nonmetallic film found in vapor region of Group I L nickel specimen 51. 500X. (b) Semimetallic bright film found in salt region of Group I high-purity nickel specimen 39. Note intergranular attack. Surface was nickel plated to preserve corrosion product. 250X.

Table 5. Surface Films Found on Group I Volatility Pilot Plant Fluorinator Test Specimens

Specimen No.	Specimen Description	Region	Gray Nonmetallic Film Maximum Thickness (mils)	Bright Semimetallic Film Maximum Thickness (mils)
51B	L nickel	Vapor	Intermittent, 3.5	Nil
		Interface	Nil	Intermittent, 1.5
		Salt	Nil	Intermittent, 1.0
51W	INCO-61 weld	Vapor	Nil	Nil
		Interface	Nil	Intermittent, 0.5
		Salt	Nil	Continuous, 1.5[a]
39	High-purity nickel	Vapor	Intermittent, 2.7	Nil
		Interface	Nil	Intermittent, 1.0
		Salt	Nil	Continuous, 1.2[b]
32	E nickel 98 Ni–2 Mn	Vapor	Intermittent, 1.2	Intermittent, 0.4
		Interface	Intermittent, 1.5	Intermittent, 0.2
		Salt	Nil	Intermittent, 0.2
24R	95 Ni–5 Fe	Vapor	Nil	Intermittent, 0.3
		Interface	Intermittent, 0.3	Intermittent, 0.2
		Salt	Nil	Intermittent, 1.0
27	90 Ni–10 Fe	Vapor	Intermittent, 1.2	Intermittent, 0.1
		Interface	Nil	Intermittent, 0.1
		Salt	Nil	Intermittent, 0.8
29	80 Ni–20 Fe	Vapor	Intermittent, 0.5	Intermittent, 0.2
		Interface	Nil	Intermittent, 0.7
		Salt	Nil	Intermittent, 0.2

[a]Semimetallic film was continuous only on one side of longitudinal section.

[b]Semimetallic film was continuous over 60% of transverse section.

Table 6. Surface Films Found on Group II Volatility Pilot Plant Fluorinator Test Specimens

Specimen No.	Specimen Description	Region	Gray Nonmetallic Film Maximum Thickness (mils)	Bright Semimetallic Film Maximum Thickness (mils)
52B	L nickel conditioned	Vapor	Intermittent, 1.0	Intermittent, 0.1
		Interface	Intermittent, 0.3	Intermittent, 0.2
		Salt	Intermittent, 0.7	Nil
52W	INCO-61 conditioned	Vapor	Intermittent, 1.3	Nil
		Interface	Intermittent, 0.5	Intermittent, 0.2
		Salt	Nil	Nil
55B	L nickel not conditioned	Vapor	Nil	Intermittent, 0.4
		Interface	Nil	Intermittent, 0.4
		Salt	Nil	Intermittent, 0.2
55W	INCO-61 not conditioned	Vapor	Intermittent, 0.4	Intermittent, 0.4
		Interface	Intermittent, 0.2	Nil
		Salt	Intermittent, 0.2	Nil
17	95 Ni–5 Co	Vapor	Intermittent, 1.8	Intermittent, 0.7
		Interface	Nil	Nil
		Salt	Nil	Nil
21	90 Ni–10 Co	Vapor	Nil	Nil
		Interface	Intermittent, 0.5	Nil
		Salt	Nil	Nil
1R	99 Ni–1 Al	Vapor	Nil	Intermittent, 0.1
		Interface	Intermittent, 0.5	Intermittent, 0.3
		Salt	Intermittent, 0.4	Nil
5	97 Ni–3 Al	Vapor	Intermittent, 0.7	Intermittent, 0.9
		Interface	Nil	Nil
		Salt	Nil	Intermittent, 0.2

Table 7, indicated the gray nonmetallic film was mostly NiF_2, while the bright semimetallic film was largely a mixture of NiO and nickel metal.

Table 7. X-Ray Diffraction Analysis of Surface Films from L Nickel Specimen 51

Surface Film			
Type	Location	Identified[a]	Line Intensity
Gray, nonmetallic	Vapor region	NiF_2	Strong
		NiO	Weak
		LiF	Weak
Bright, semimetallic	Salt region	NiO	Medium
		Ni	Medium

[a]Unidentified extra lines also present in both samples.

Surface Attack

Many of the corrosion specimens examined showed an attack of varying character which generally could not be categorized under any heading except surface attack. Occasionally this surface attack had the appearance of pitting-type corrosion. Some typical examples of the types of surface attack found are shown in Fig. 8. Additional photomicrographs showing surface attack are presented in the Appendix.

Intergranular Attack

Intergranular attack was found in many samples from the corrosion specimens. Figure 7 illustrates this mode of corrosion as found on L nickel. The amount of intergranular attack observed on all specimens is recorded in Tables 8 and 9. In all cases corrosion resembling intergranular attack was designated as such only if the attack was observed in the "as-polished" metallographic condition.

Grain-Boundary Modifications

In some of the fluorinator specimens, grain-boundary modifications occurred which differed from intergranular attack as previously defined. This form of grain-boundary attack was not apparent in the "as-polished" metallographic sections as was the case for intergranular attack, but was

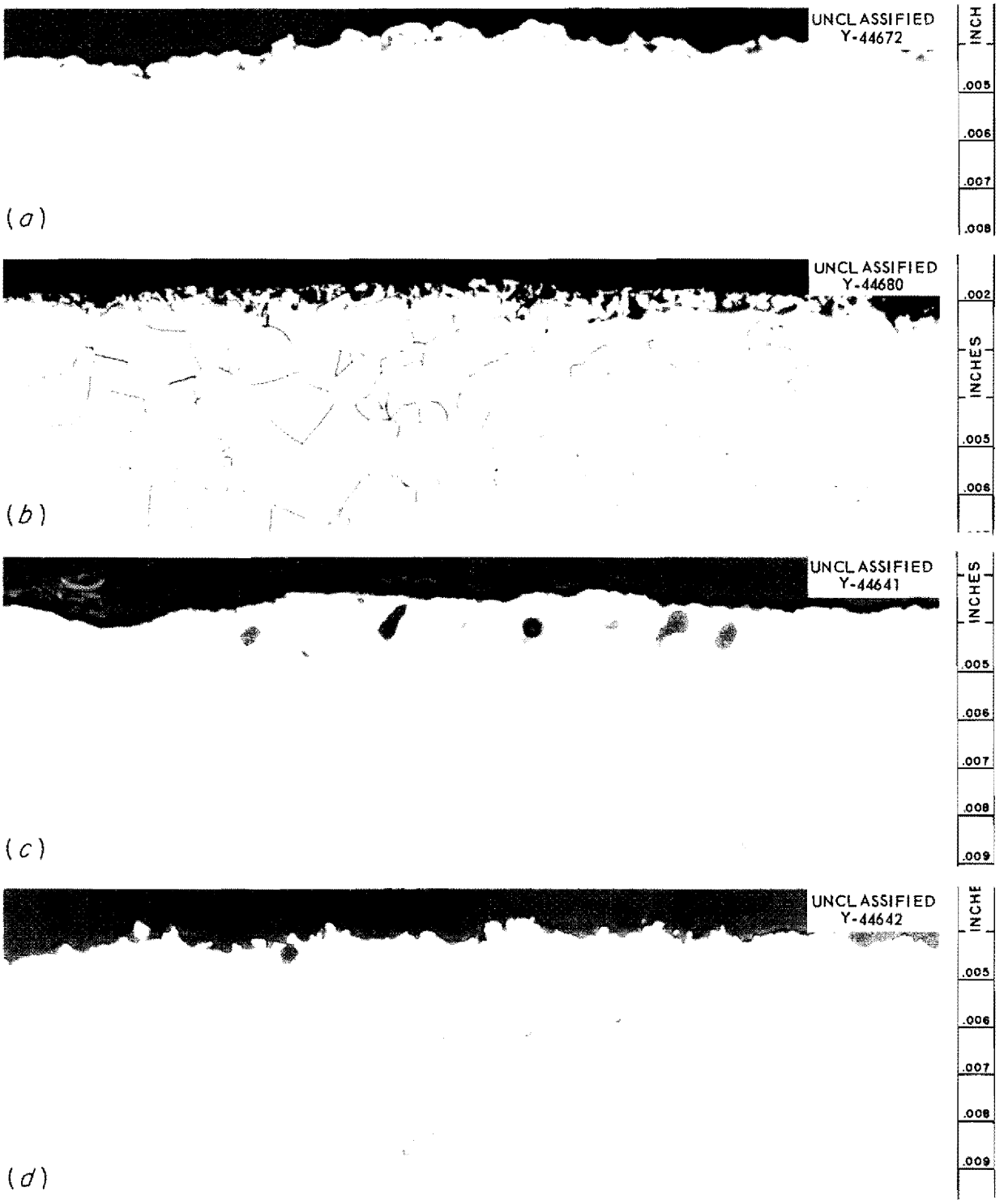

Fig. 8. Surface Attack Found on Volatility Pilot Plant Fluorinator Test Specimens, Group II. (a) Vapor region of 99 Ni–1 Al specimen 1R. (b) Vapor region of 97 Ni–3 Al specimen 5. (c) Vapor region of conditioned INCO-61 weld of specimen 52. (d) Interface region of conditioned INCO-61 weld of specimen 52. 300X.

Table 8. Corrosion of Group I Volatility Pilot Plant Fluorinator Test Specimens

Specimen No.	Material	Region	Maximum Bulk Metal Attack (mils)	Maximum Surface Attack (mils)	Maximum Intergranular Attack (mils)	Total Attack (mils)
51	L nickel conditioned	Vapor	0.7	0.5		1.2
		Interface	1.0		1.5	2.5
		Salt	1.1		4.5	5.6
51 weld	INCO-61 conditioned	Vapor	1.3			1.3
		Interface	1.1	0.2		1.3
		Salt	1.2		2.0	3.2
39	High-purity nickel	Vapor	1.0	0.2		1.2
		Interface	1.6		5.0	6.6
		Salt	0.7		6.5	7.2
32	E nickel 98 Ni–2 Mn	Vapor	1.0	0.3		1.3
		Interface	1.0			1.0
		Salt	0.9			0.9
24R	95 Ni–5 Fe	Vapor	0.9	0.5		1.4
		Interface	0.7	0.1		0.8
		Salt	1.1	0.7		1.8
27	90 Ni–10 Fe	Vapor	1.0	0.3		1.3
		Interface	0.9	0.3		1.2
		Salt	0.9	0.3		1.2
29	80 Ni–20 Fe	Vapor	1.5	0.7		2.2
		Interface	0.7	1.0		1.7
		Salt	1.0	0.7		1.7

Table 9. Corrosion of Group II Volatility Pilot Plant Fluorinator Test Specimens

Specimen No.	Material	Region	Maximum Bulk Metal Attack (mils)	Maximum Surface Attack (mils)	Maximum Intergranular Attack (mils)	Total Attack (mils)
52	L nickel conditioned	Vapor	1.5		2.0	3.5
		Interface	4.6		3.0	7.6
		Salt	3.6		4.5	8.1
52 weld	INCO-61 conditioned	Vapor	2.7	1.0		3.7
		Interface	6.1	0.5		6.6
		Salt	6.7			6.7
55	L nickel not conditioned	Vapor	1.4		3.0	4.4
		Interface	5.7		6.0	11.7
		Salt	3.6		5.0	8.6
55 weld	INCO-61 not conditioned	Vapor	2.0	0.2		2.2
		Interface	6.8			6.8
		Salt	3.7			3.7
17	95 Ni–5 Co	Vapor		1.0		1.0
		Interface	6.7		4.5	11.2
		Salt	6.0		5.0	11.0
21	90 Ni–10 Co	Vapor	2.1			2.1
		Interface	8.2			8.2
		Salt	6.5		0.3	6.8
1R	99 Ni–1 Al	Vapor	1.2	0.5		1.7
		Interface	5.8			5.8
		Salt	3.9			3.9
5	97 Ni–3 Al	Vapor	1.8	0.9		2.7
		Interface	8.6		0.5	9.1
		Salt	4.2			4.2

visible when the sections were etched with 3 parts CH_3COOH and 2 parts HNO_3. The modifications were found to be more clearly defined if the etched surface was then lightly repolished on a microcloth wheel using 0.1 μ alumina (see Fig. 9a). Another standard etchant for nickel, 92 $HCl:5H_2SO_4:3HNO_3$, revealed only the normal structure usually observed on nickel (Fig. 9b).

The depth of grain-boundary modifications present in the Volatility Pilot Plant specimens was determined using the nitric-acetic acid etch-and-repolish technique described above.

The maximum depth of these grain-boundary modifications for each corrosion specimen is recorded in Tables 10 and 11. The maximum amount of grain-boundary modifications was usually observed in the sections taken from the salt regions. For high-purity nickel, the depth of the grain-boundary modifications was found to increase in proportion to the distance from the top of the specimen (see Fig. 10).

Bend Tests

In order to gain preliminary information on how deleterious the grain-boundary modifications were on the properties of the fluorination specimens, a few bend tests were performed on the high-purity nickel samples. This material was selected because samples had shown grain-boundary modifications with and without accompanying intergranular attack. Details of the test and the results are shown in Table 12. Fracturing occurred in specimens showing the modifications whether or not intergranular attack accompanied the modifications. However, the depth of the modifications did not seem to affect the depth of the 180-deg bend fractures.

Summary

The maximum total corrosion of the Volatility Pilot Plant specimens was determined in two ways:

1. By summing the bulk metal losses, surface attack, and intergranular attack.

2. By summing the bulk metal losses and the grain-boundary modifications. Maximum values for each mode of attack were used in all cases.

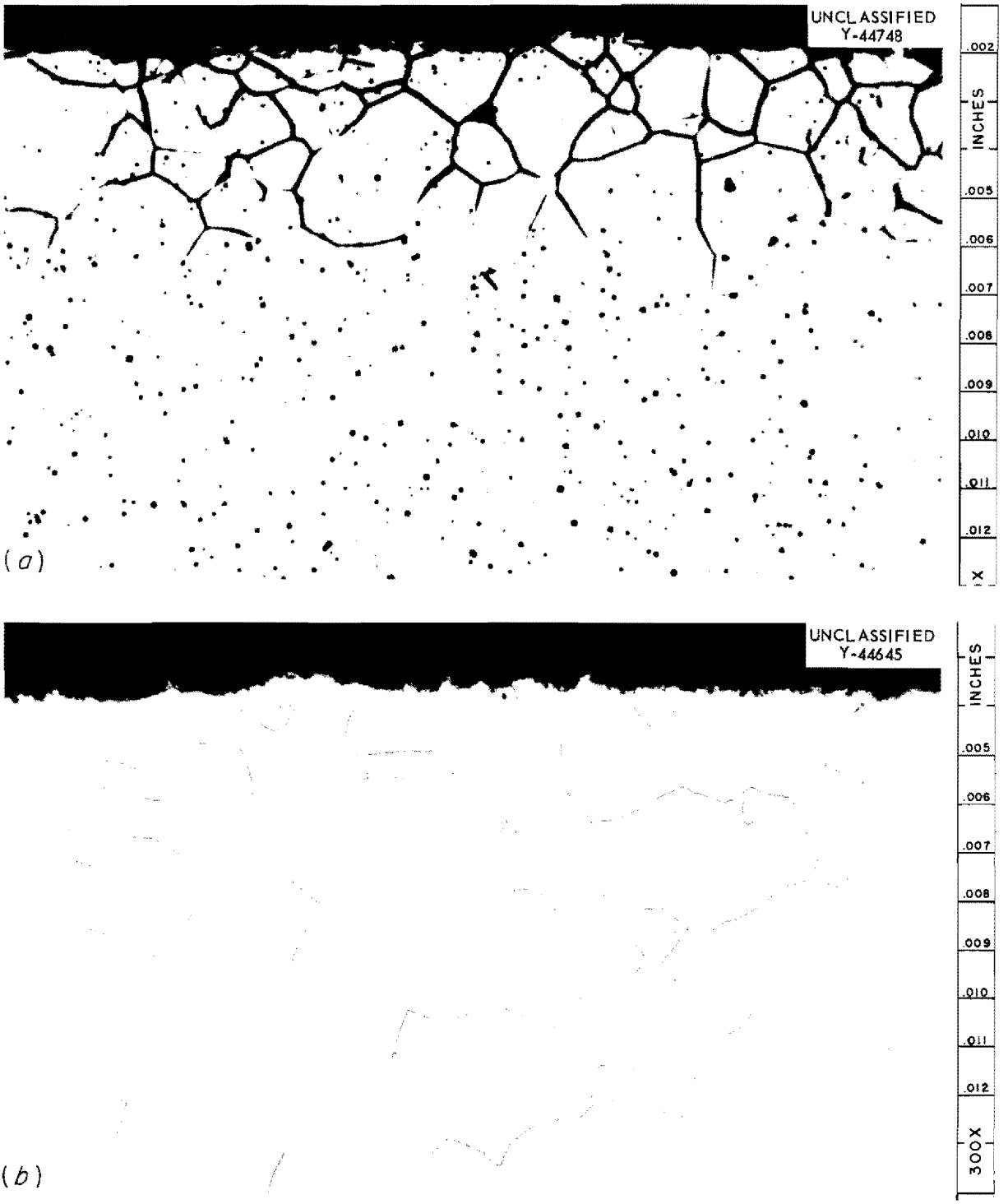

Fig. 9. Development of Grain-Boundary Modifications in L Nickel by Etching. Specimen 52B – vapor region. (a) Etched with $3CH_3COOH:2HNO_3$ and repolished. (b) Etched with $92HCl:5H_2SO_4:3HNO_3$.

Table 10. Grain-Boundary Modifications in Group I Volatility Pilot Plant Fluorinator Test Specimens

Specimen No.	Material	Region	Grain-Boundary Modifications[a] (mils)
51	L nickel conditioned	Vapor	1.5
		Interface	9.5
		Salt	11.5
51 weld	INCO-61 conditioned	Vapor	0
		Interface	0
		Salt	0
39	High-purity nickel	Vapor	12
		Interface	28
		Salt	125
32	E nickel 98 Ni–2 Mn	Vapor	0
		Interface	2
		Salt	3.5
24R	95 Ni–5 Fe	Vapor	none apparent[b]
		Interface	
		Salt	
27	90 Ni–10 Fe	Vapor	0
		Interface	6
		Salt	10
29	80 Ni–20 Fe	Vapor	2[c]
		Interface	5
		Salt	5

[a]Except where noted, measurements are for transverse sections.

[b]Etching behavior may have masked grain-boundary modifications.

[c]Measured in longitudinal section.

Table 11. Grain-Boundary Modifications in Group II Volatility Pilot Plant Fluorinator Test Specimens

Specimen No.	Material	Region	Grain-Boundary Modifications[a] (mils)
52	L nickel conditioned	Vapor	5.5
		Interface	5.5
		Salt	7
52 weld	INCO-61 conditioned	Vapor	0
		Interface	0
		Salt	0
55	L nickel not conditioned	Vapor	6
		Interface	4.5
		Salt	7
55 weld	INCO-61 not conditioned	Vapor	0
		Interface	0
		Salt	0
17	95 Ni–5 Co	Vapor	3.5
		Interface	30
		Salt	39
21	90 Ni–10 Co	Vapor	4
		Interface	3.5
		Salt	5
1R	99 Ni–1 Al	Vapor	none apparent[b]
		Interface	
		Salt	
5	97 Ni–3 Al	Vapor	0
		Interface	15.5
		Salt	14.5

[a] Measurements are for transverse sections.

[b] Etching behavior may have masked grain-boundary modifications.

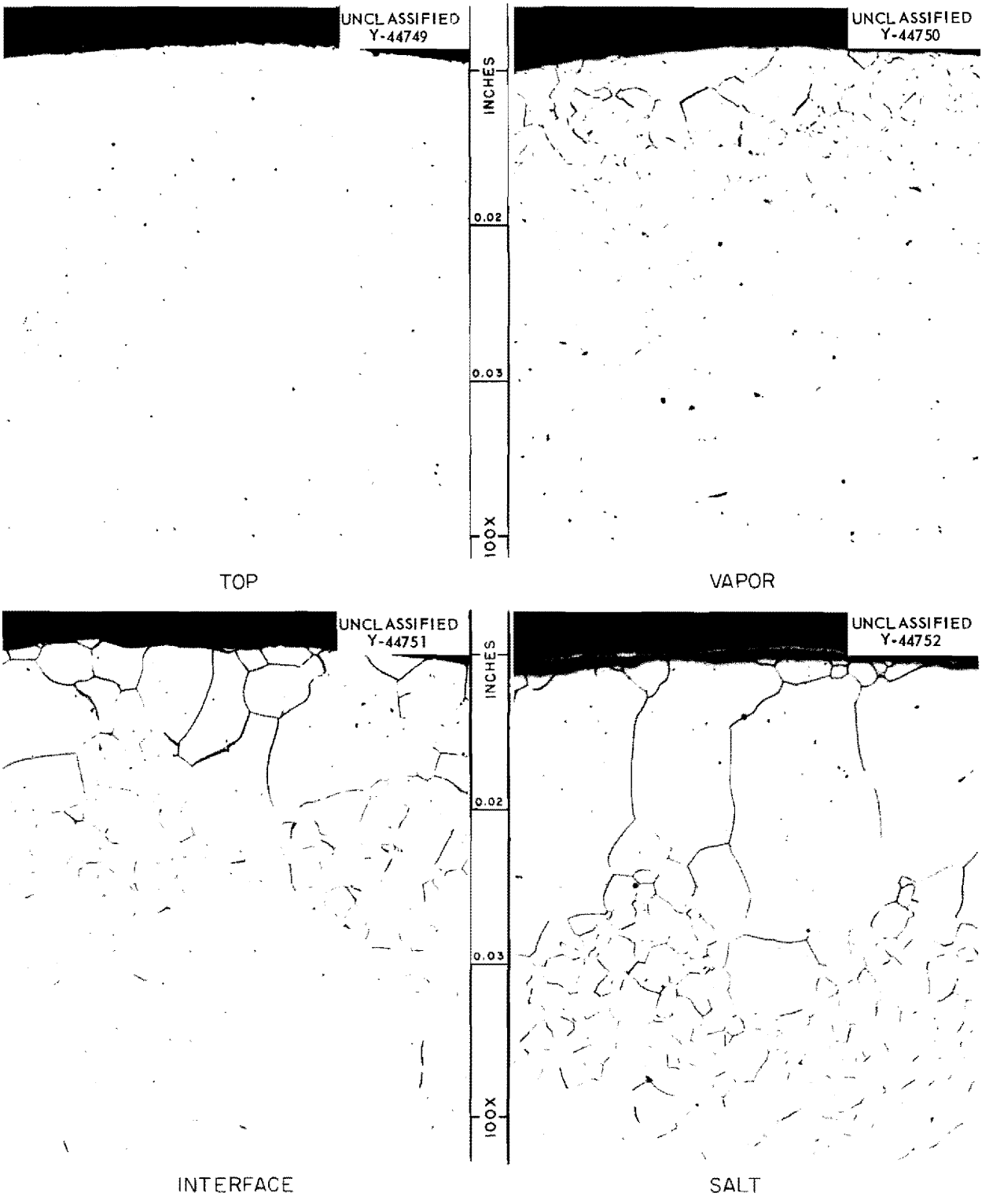

Fig. 10. Grain-Boundary Modifications in High-Purity Nickel Specimen 39. Etched with $3CH_3COOH:2HNO_3$ and repolished lightly on a microcloth wheel using 0.1-μ alumina.

Table 12. Grain-Boundary Modifications on Bend-Test Fracture of High-Purity Nickel

Location	Maximum Depth of Intergranular Attack (mils)	Maximum Depth of Grain-Boundary Modifications (mils)	Maximum Depth of Fracturing After 180-deg Bend (mils)
Top	0	0	0
Vapor	0	12	15
Salt	6.5	125	9

Bulk losses based on specimen radii were used since aggressive attack on a process fluorinator occurs essentially only on the inside diameter. Total corrosion noted for the specimens is detailed in Tables 8 and 9. Corrosion rates for the fluorination specimens are shown in Figs. 11 and 12. The rates were determined on the basis of molten-salt residence time as well as fluorine exposure time.

DISCUSSION OF RESULTS

The individual effects of fluorine, UF_6, and fluoride salts on container materials have been discussed previously.[5] The modes of attack observed in this current series were similar to those previously described. However, attempts were made to categorize better the corrosion modes.

Comparison Between Group I and Group II Specimens

The Group II corrosion specimens in general exhibited higher corrosion rates than did the Group I specimens, probably due to the presence of uranium during the Group II runs. Previous work has shown the accelerating effect uranium has on corrosion during fluorination.[5]

Bulk metal losses, based on specimen radii, were about the same, 0.7 to 1.6 mils, for all the Group I specimens while the metal losses for the

[5]A. P. Litman and A. E. Goldman, Corrosion Associated with Fluorination in the Oak Ridge National Laboratory Fluoride Volatility Process, ORNL-2832, pp 25–31 (June 5, 1961).

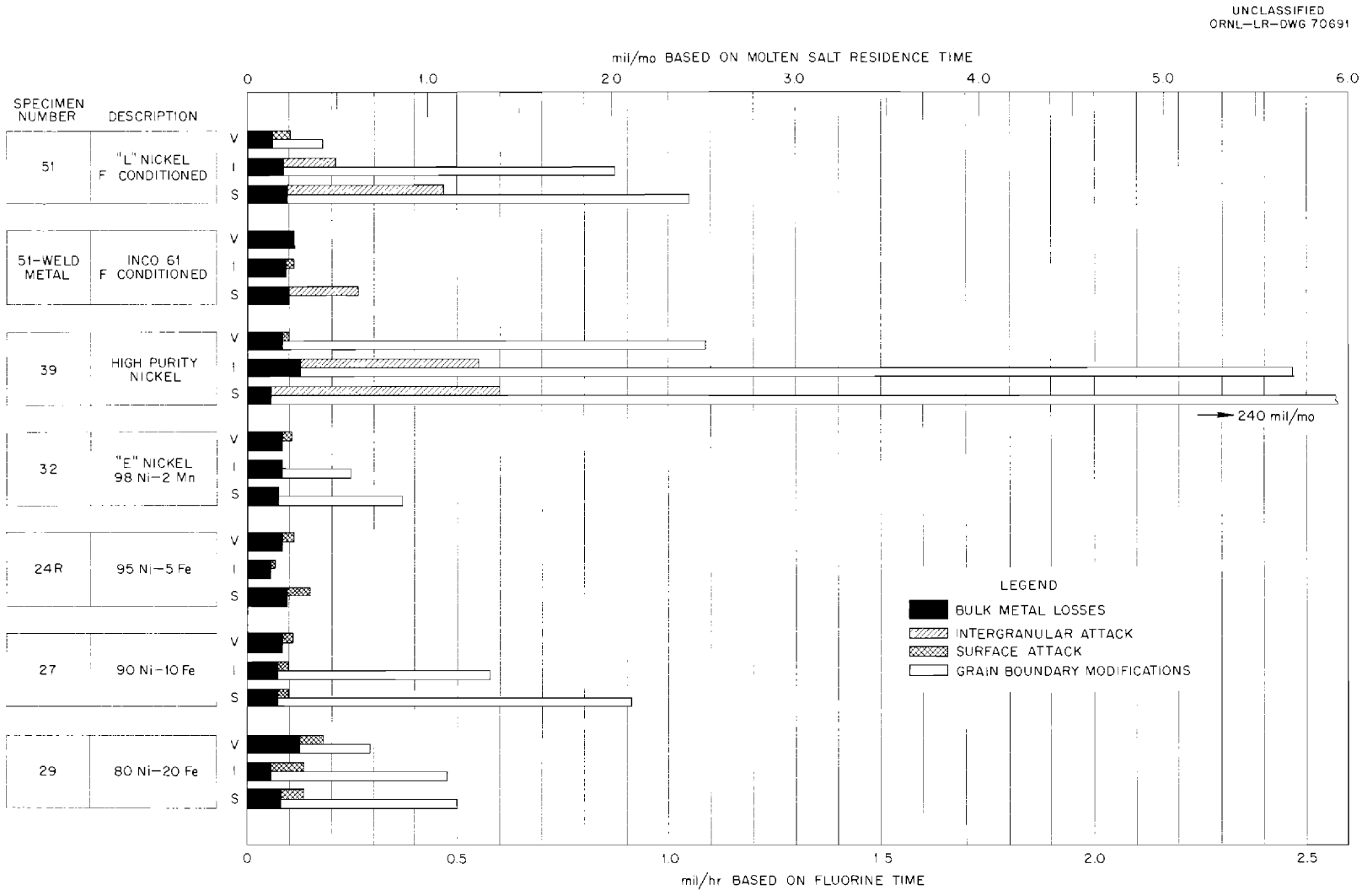

Fig. 11. Corrosion Rates for Group I Volatility Pilot Plant Fluorinator Test Specimens.

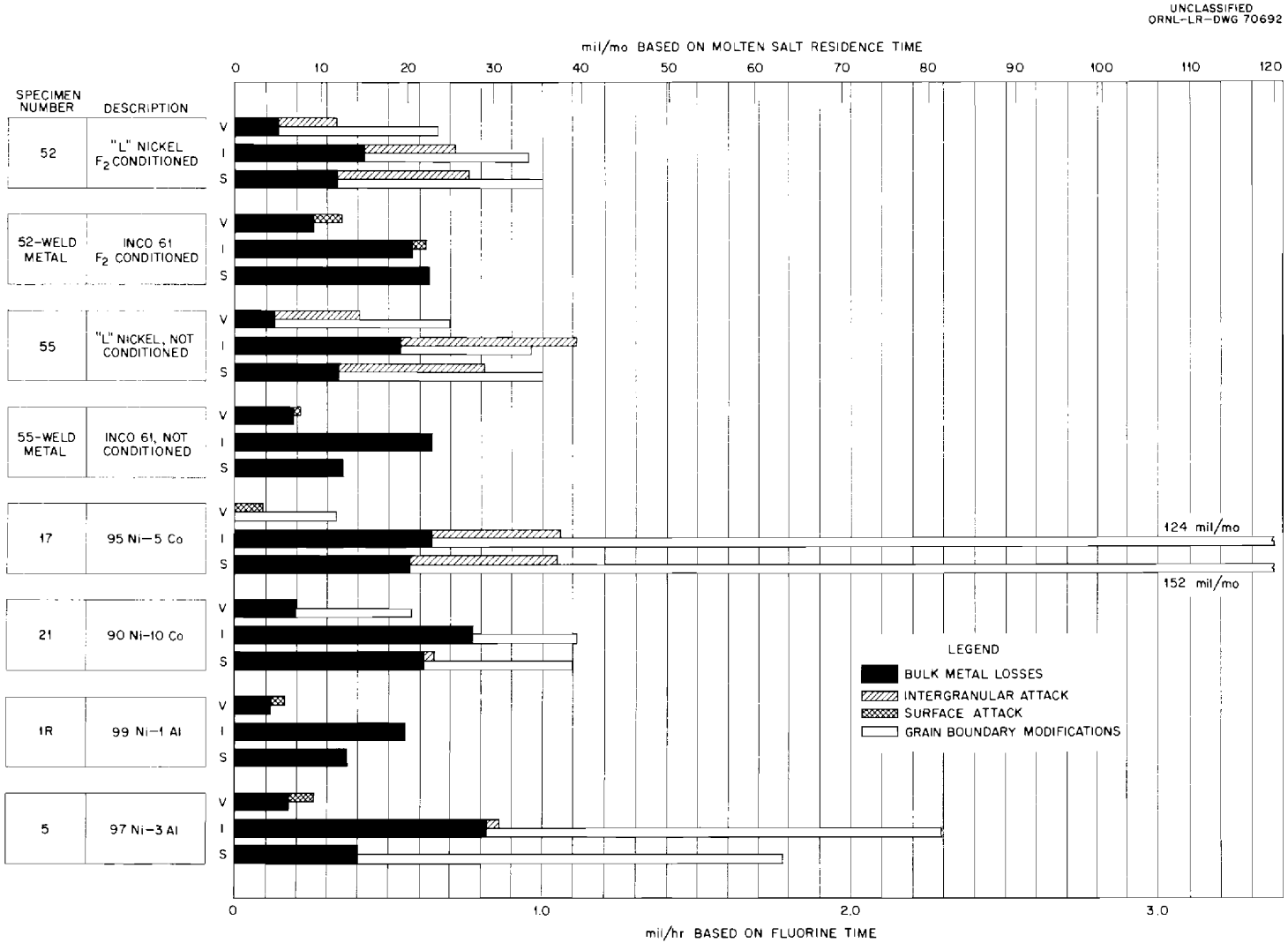

Fig. 12. Corrosion Rates for Group II Volatility Pilot Plant Fluorinator Test Specimens.

Group II specimens varied from 0 to 8.6 mils. Group II interface sections usually exhibited the greatest bulk losses, while sections taken in the vapor region exhibited the least attack.

Intergranular attack was most prominent in the L nickel and high-purity nickel specimens of Group I. The maximum depth of penetration by this mode of attack was 6.5 mils for the high-purity nickel specimen.

In Group II, intergranular attack was found mainly in the L nickel and 95 Ni–5 Co specimens. For the unconditioned L nickel specimen, intergranular attack to a depth of 6 mils was noted.

Grain-boundary modifications were found in all specimens of Group I except INCO-61 weld metal and 95 Ni–5 Fe specimens. The L nickel and high-purity nickel specimens showed the greatest amount of grain-boundary modifications – 11.5 and 125 mils, respectively.

All the Group II specimens except the INCO-61 weld metal and the 99 Ni–1 Al specimens exhibited grain-boundary modifications. The maximum depth of attack by this mode of corrosion, 30 mils, was found in the 95 Ni–5 Co specimen.

Comparison With Previous Studies

In general, the corrosion rates experienced by the Group I and Group II specimens were about the same as those experienced by specimens in earlier tests.[5] Since many different alloys were tested in the current and previous series, the best comparison can be made by examining corrosion of the L nickel control specimens. Table 13 gives the maximum corrosion rates experienced by all such nickel specimens.

As Table 13 indicates, during corrosion tests the L nickel specimens were exposed in $NaF-ZrF_4$ salts (usually with UF_4 present), while the Group I/Group II tests were exposed to a $LiF-NaF-ZrF_4$ mixture. The addition of LiF lowered the salt melting point so that the fluorination could proceed at slightly lower temperatures. The lower operating temperatures would normally decrease corrosion rates. However, as has been shown previously, the addition of lithium fluoride increases the corrosion rates on nickel[5] and the total effect was one of averaging so that composite corrosion rates were about the same as in the early tests.

Table 13. Comparison Between Maximum Corrosion Rates Experienced by L Nickel Specimens in Group I/Group II Tests and in Corrosion Tests

Tests	Runs	Approximate Temperature Range (°C)	Initial Bath Composition (mole %)	Maximum Corrosion Rate	
				Based on Salt Residence Time (mils/month)	Based on Fluorine Time (mils/hr)
Corrosion tests	M 21–M 48	505–700	50 NaF–50 ZrF_4	> 100[a]	> 4.0[a]
	C 9–C 15	500–650	48 NaF–48 ZrF_4–4 UF_4	72	1.2
	E 3–E 6	540–660	48 NaF–49.5 ZrF_4–2.5 UF_4	45	0.8
	L 1–L 4	560–710	54 NaF–41 ZrF_4–5 UF_4	74	1.5
	L 5–L 9	540–700	52 NaF–45.5 ZrF_4–2.5 UF_4	27	0.7
Group I	T 1–T 7	485–605	30 LiF–27 NaF–43 ZrF_4	11[b]	0.5[b]
Group II	TU 1–TU 7	490–575	29 LiF–29 NaF–42 ZrF_4 + 0.3 wt % U[c]	40	1.1

[a]Specimen was completely consumed.

[b]Specimen was fluorine conditioned 3.2 hr at 600–645°C before test. All other specimens were in unconditioned state.

[c]Equivalent to 0.2 mole % U.

Effect of Fluorine Conditioning on L Nickel and INCO-61 Weld Metal

In Group II, one of the L nickel-INCO 61 specimens was fluorine conditioned 3.2 hr at 600–645°C before corrosion testing. The conditioned L nickel appeared to have sustained somewhat less attack than unconditioned L nickel. On the other hand, conditioned INCO-61 weld metal exposed in the vapor and salt regions exhibited greater attack than did unconditioned INCO 61.

These observations are compatible with the theory that corrosion resistance to fluorine is imparted by the formation of a stable fluoride film. The increased corrosion resistance of the conditioned L nickel presumably is due to the formation of a stable nickel fluoride film. The titanium present in INCO 61 possibly modifies and makes the NiF_2 film less stable since titanium fluorides are highly volatile.

CONCLUSIONS

Several conclusions can be drawn based on the reported fluorination-corrosion tests. These conclusions are in agreement with the previous test series.

1. The combination of operating temperatures around 550°C with lithium fluoride present in the salt baths produces about the same bulk metal losses on nickel and nickel-base alloys as was found by operating at 650°C without lithium in the salt baths.

2. The presence of uranium accelerates corrosion of nickel and nickel-base alloys during the Volatility Process fluorination cycle.

3. Prior fluorine conditioning of L nickel decreases corrosion of the material during subsequent fluorination.

4. Prior fluorine conditioning of INCO-61 weld metal increases the attack on INCO 61 during subsequent fluorination.

5. Bulk metal losses on L nickel and the nickel-binary alloys containing manganese, iron, cobalt, or aluminum are about the same during fluorination at 550°C with lithium present in the fluoride salt baths.

6. The presence of the alloying elements, manganese, iron, or aluminum, in nickel drastically reduces or eliminates intergranular attack usually found in unalloyed nickel exposed to a fluorination environment.

7. In fluorination environments, the effect of adding cobalt to nickel on subsequent corrosion by intergranular attack of the binary is unclear. These reported tests showed that serious intergranular attack of a 95 Ni–5 Co specimen occurred. On the other hand, this test series and previous series showed good resistance to this form of corrosion by nickel containing 10 and 20 wt % Co.

8. Unalloyed nickel of greater than commercial purity shows less resistance to bulk metal losses, intergranular attack, and grain-boundary modifications when exposed to fluorination environments than L nickel and all nickel alloys tested.

ACKNOWLEDGMENT

The authors wish to acknowledge the assistance given by L. A. Amburn, Metallography Group, the X-Ray Diffraction Group, Metals and Ceramics Division, and by personnel of the Analytical Chemistry Division.

Thanks are also due E. C. Moncrief, R. P. Milford, and others of the Chemical Technology Division who aided in gathering process data or in reviewing this report.

Special thanks are due D. A. Douglas, Jr., R. S. Crouse, and R. J. Gray for their constructive appraisal of this report, and to the Metals and Ceramics Division Reports Office and Graphic Arts Department for preparation of the material for reproduction.

APPENDIX

Photomicrographs of metallographic sections taken from Groups I and II, nickel and nickel-base, corrosion specimens exposed in the Volatility Pilot Plant Mark III L nickel fluorinator.

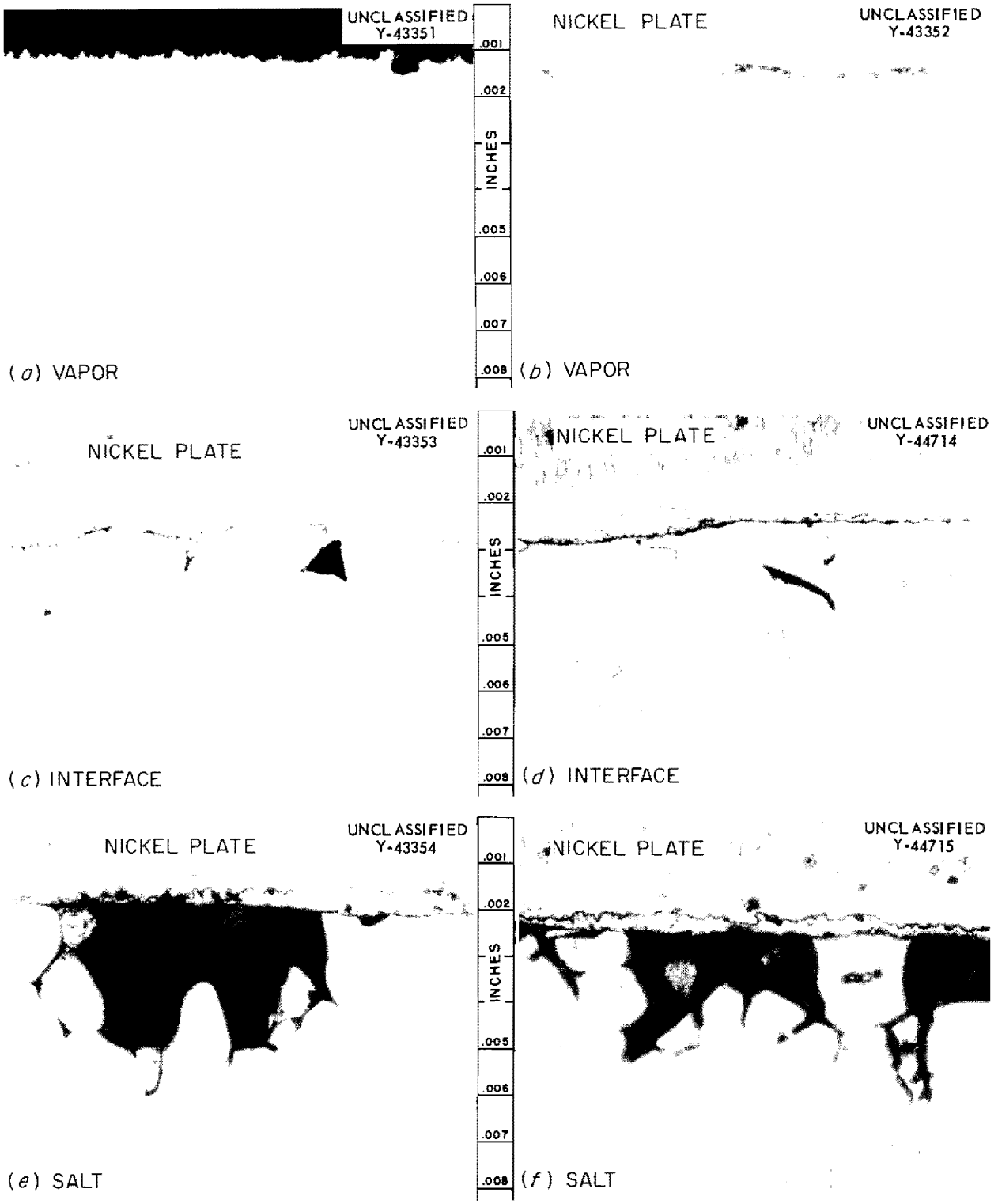

Fig. 13. Sections from L Nickel Specimen 51 from Group I, Volatility Pilot Plant Fluorinator Test Specimens. Left — as-polished; right — as-etched with HNO_3-CH_3COOH-HCl. 300X.

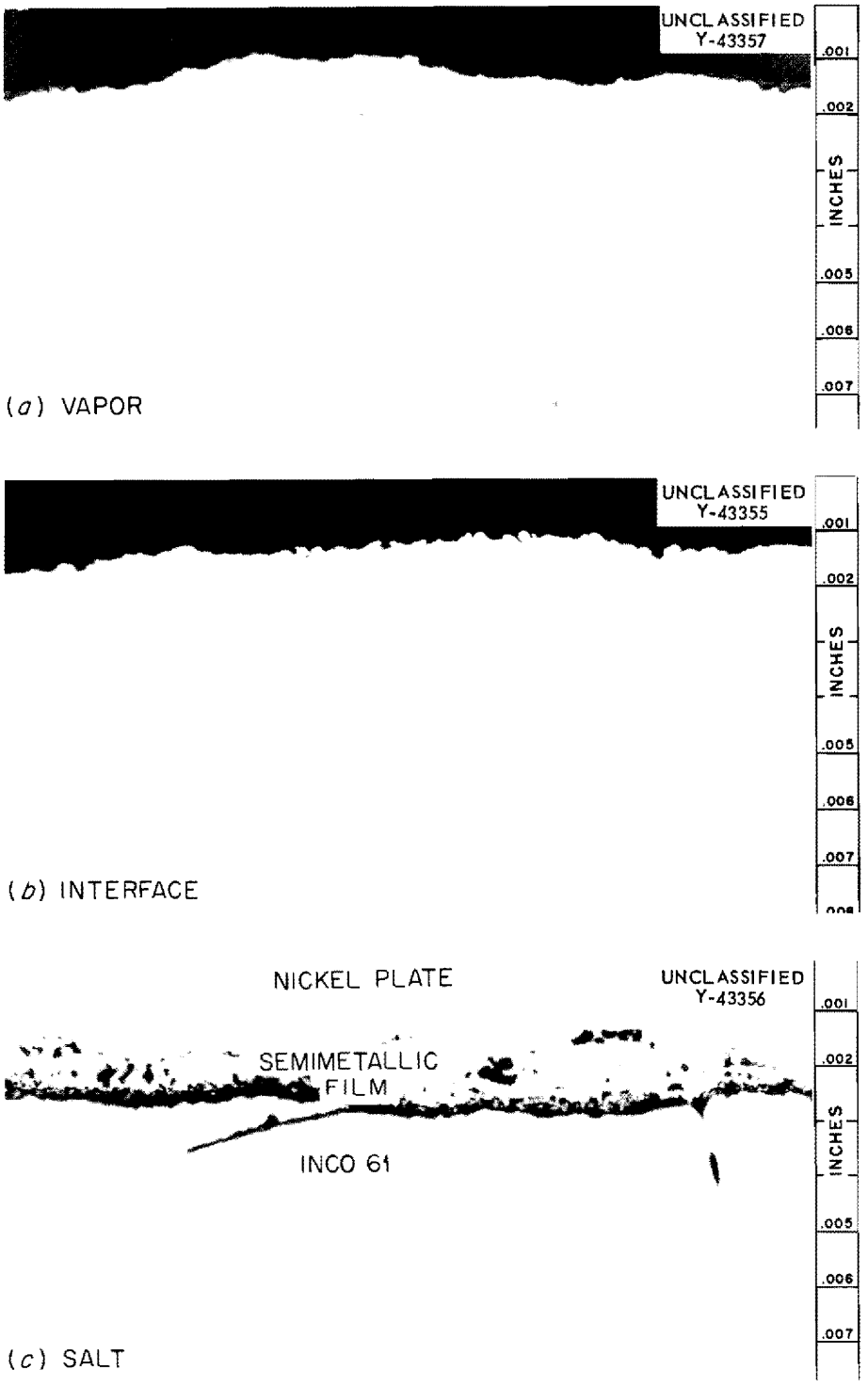

Fig. 14. Sections from INCO-61 Weld Deposit of Specimen 51 from Group I Volatility Pilot Plant Fluorinator Test Specimens. As-polished. 300X.

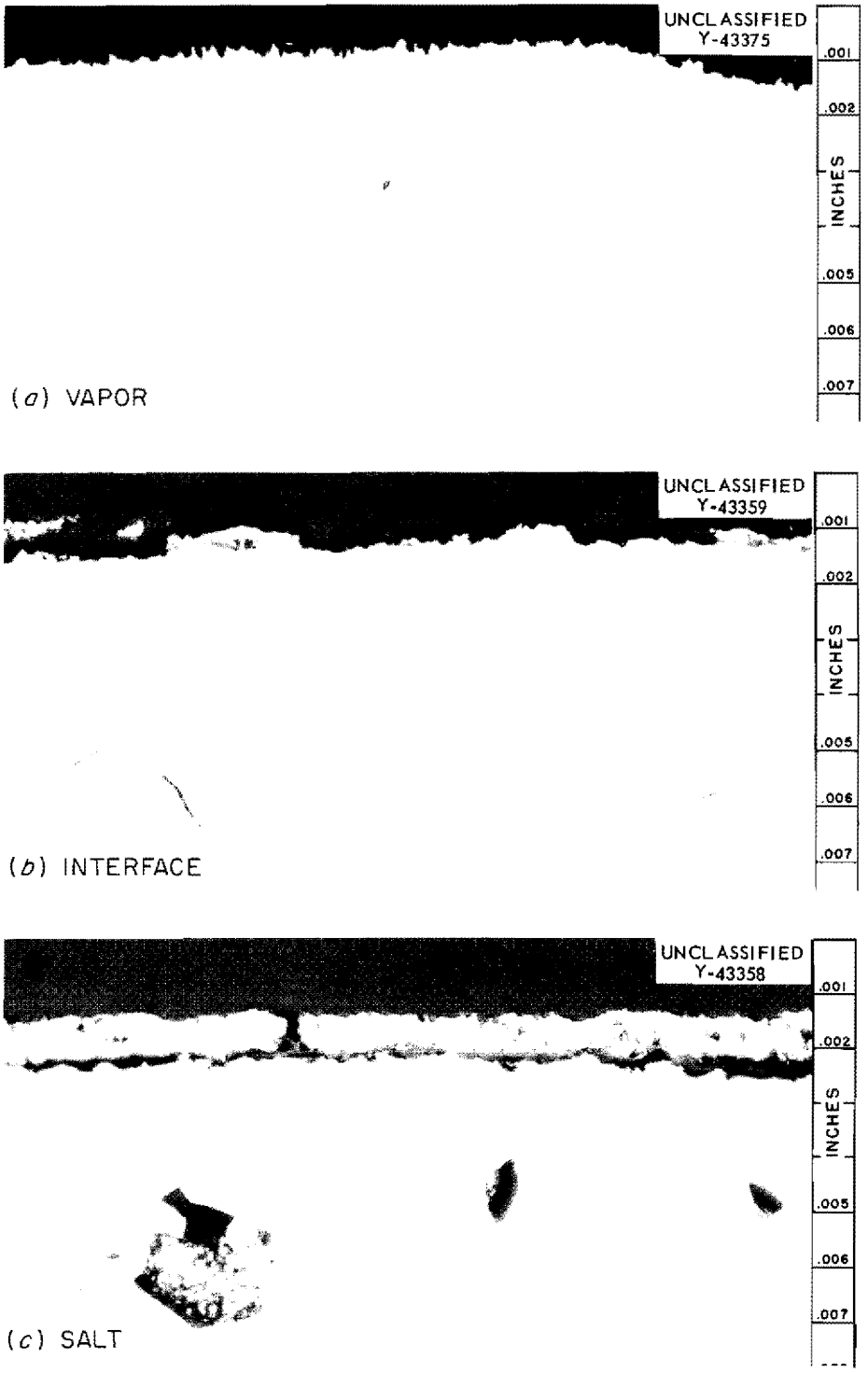

Fig. 15. Sections from High-Purity Nickel Specimen 39 from Group I Volatility Pilot Plant Fluorinator Test Specimens. As-polished. 300X.

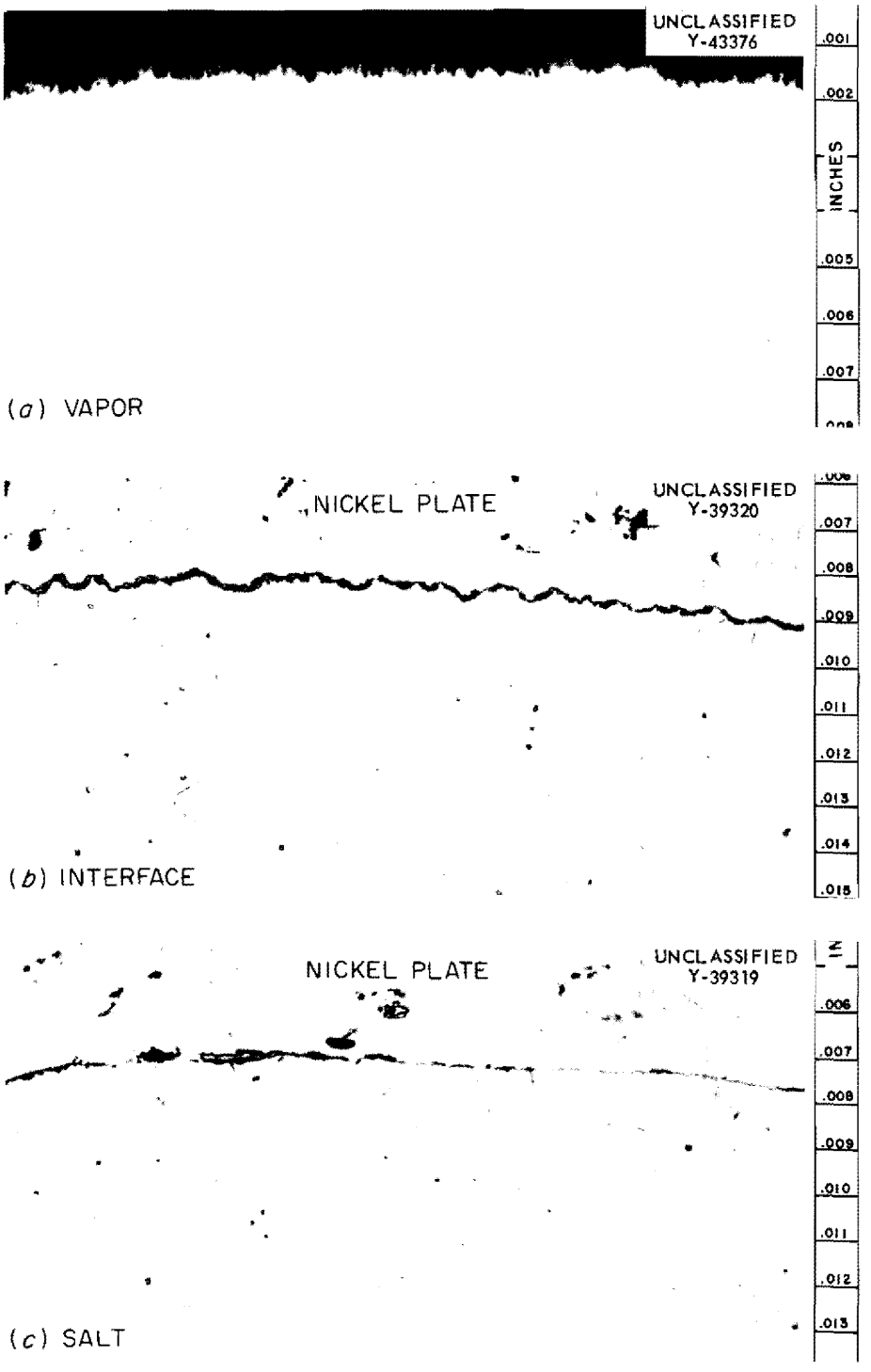

Fig. 16. Sections from 98 Ni–2 Mn Specimen 32 from Group I Volatility Pilot Plant Fluorinator Test Specimens. (a) As-polished. 300X. (b) As-etched with HNO_3-CH_3COOH-HCl. 250X. (c) As-etched with HNO_3-CH_3COOH-HCl. 250X.

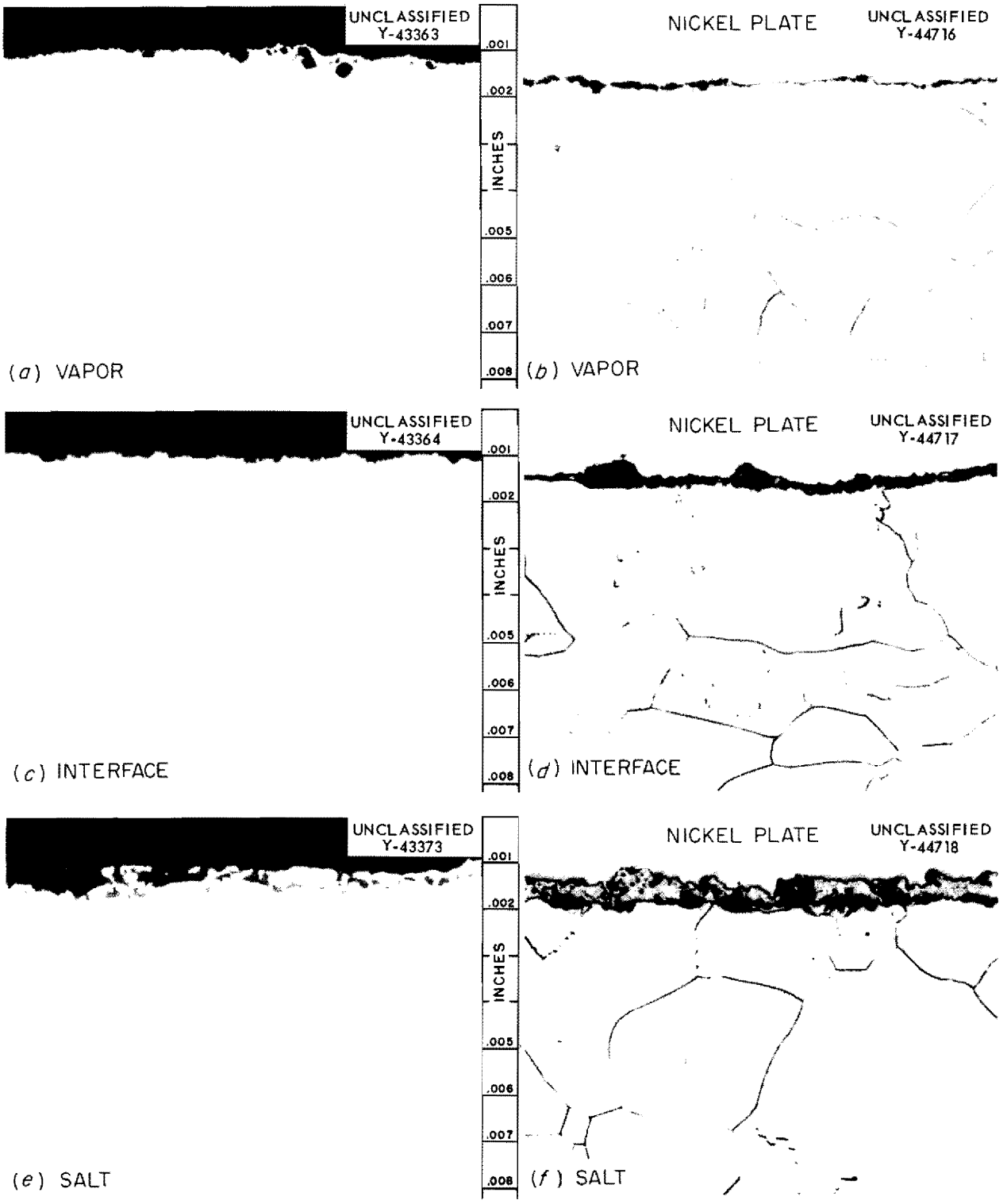

Fig. 17. Sections from 95 Ni–5 Fe Specimen 24R from Group I Volatility Pilot Plant Fluorinator Test Specimens. Left — as-polished; right — as-etched with HNO_3-CH_3COOH-HCl. 300X.

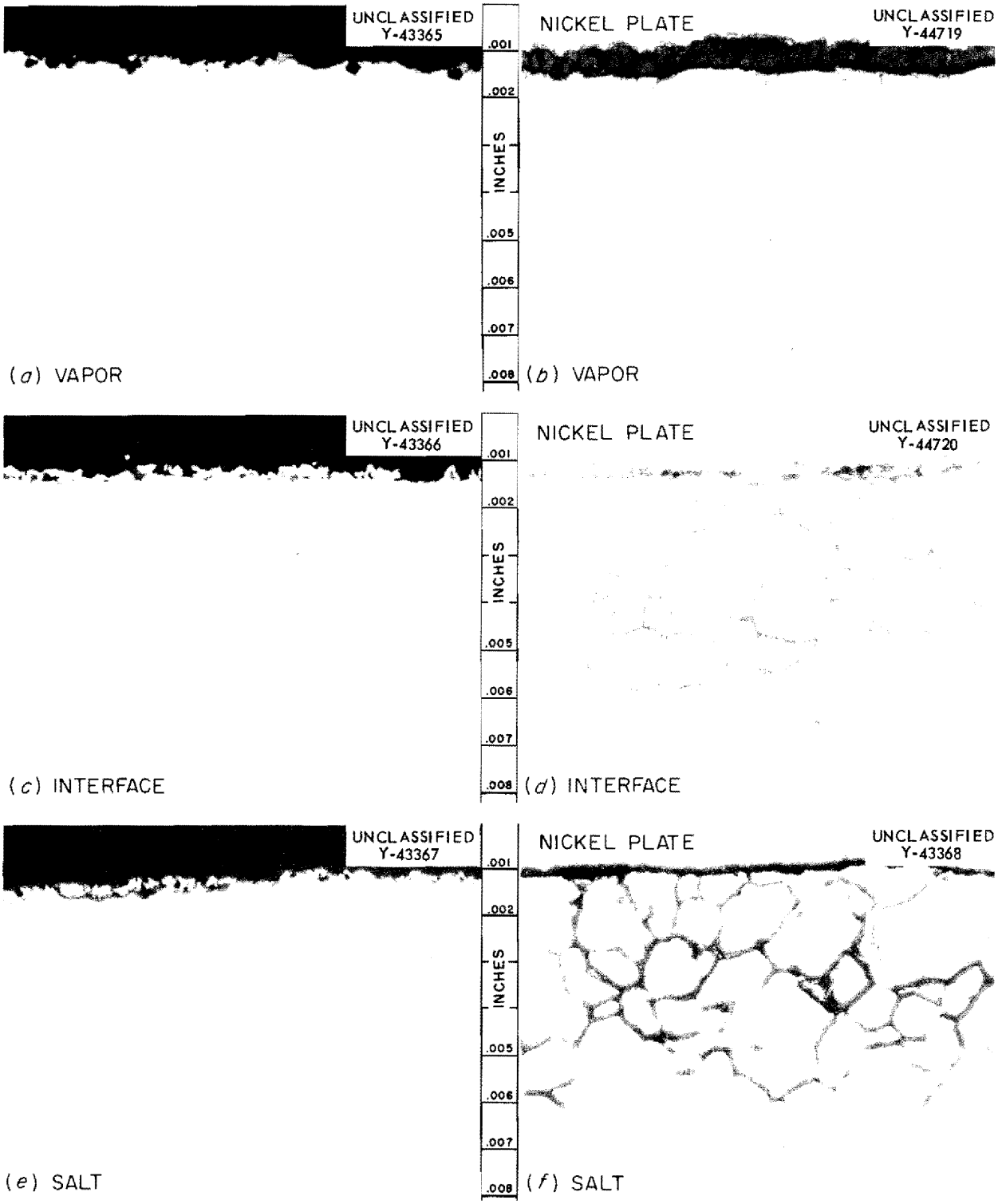

Fig. 18. Sections from 90 Ni–10 Fe Specimen 27 from Group I Volatility Pilot Plant Fluorinator Test Specimens. Left – as-polished; right – as-etched with HNO_3-CH_3COOH-HCl. 300X.

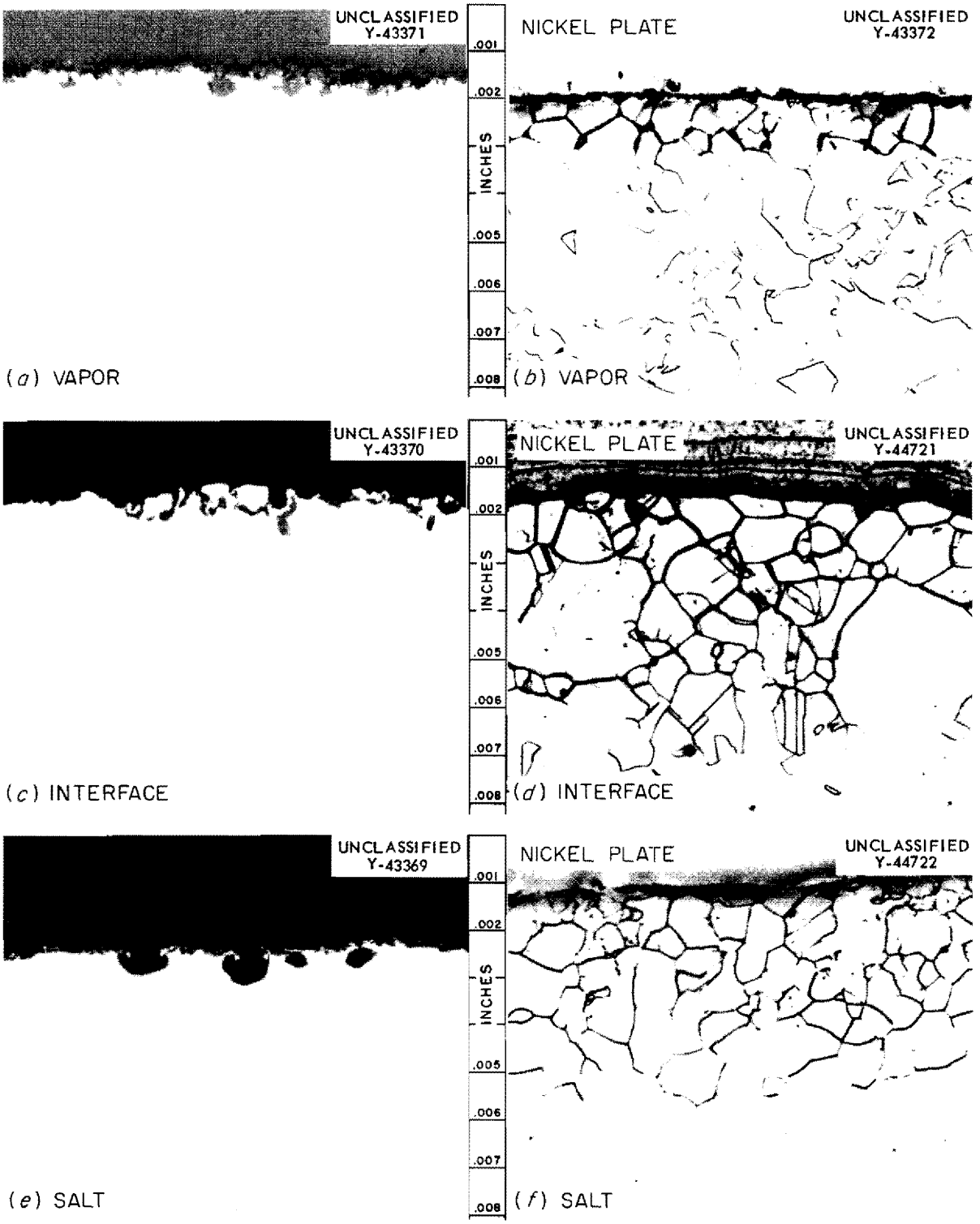

Fig. 19. Sections from 80 Ni–20 Fe Specimen 29 from Group I Volatility Pilot Plant Fluorinator Test Specimens. Left – as-polished; right – as-etched with HNO_3-CH_3COOH-HCl. 300X.

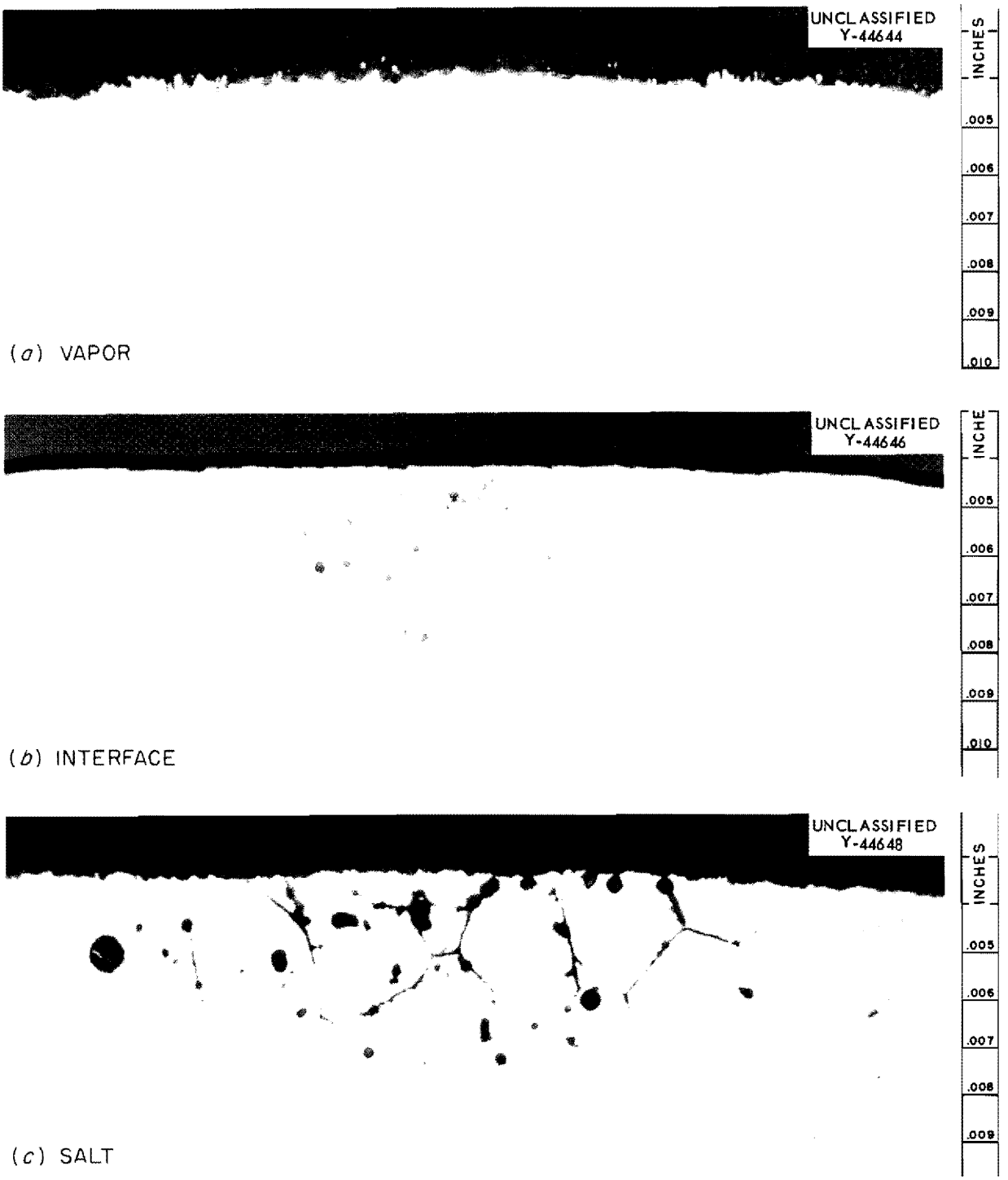

Fig. 20. Sections from L Nickel Specimen 52 from Group II Volatility Pilot Plant Fluorinator Test Specimens. As-polished. 300X.

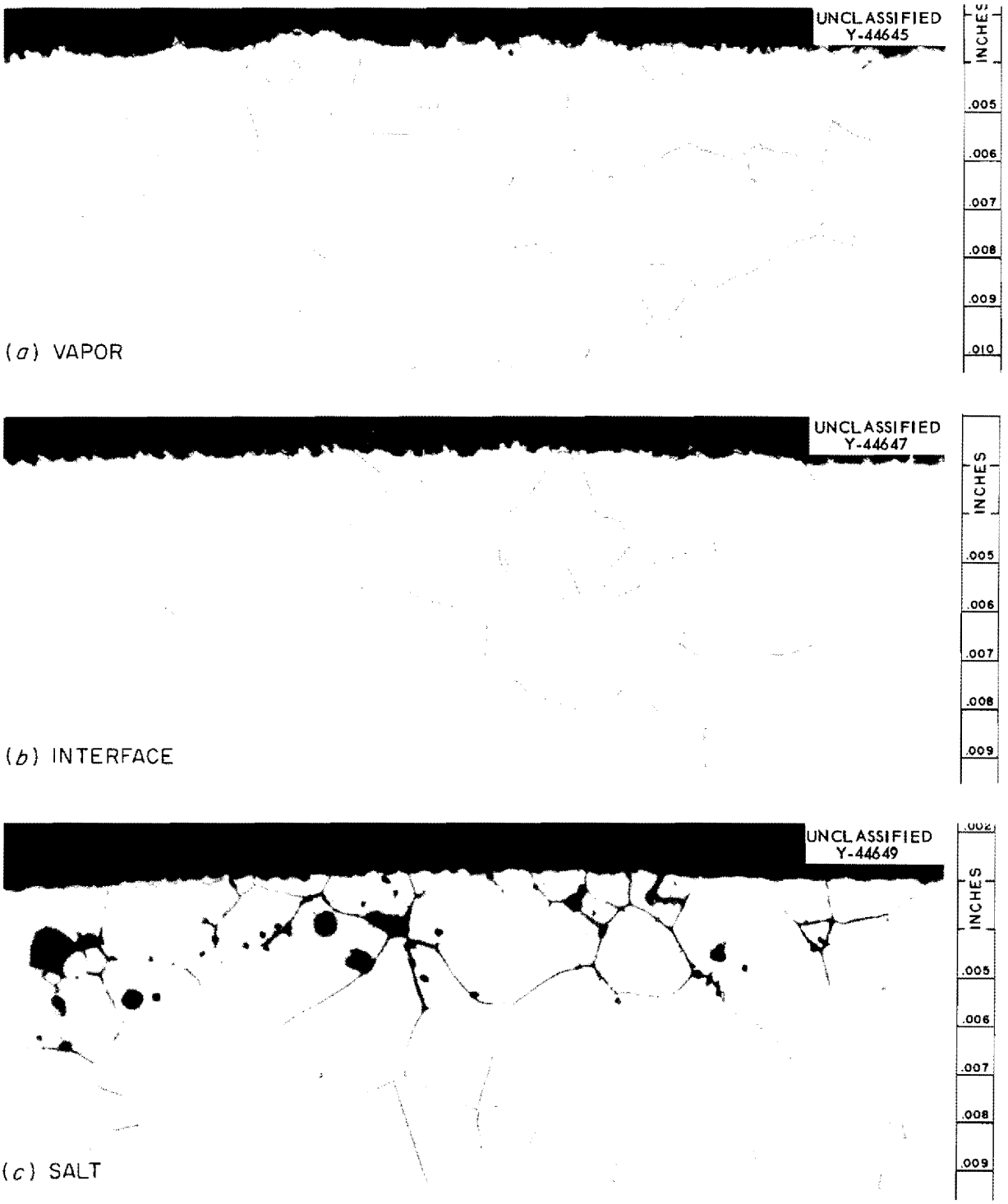

Fig. 21. Sections from L Nickel Specimen 52 from Group II Volatility Pilot Plant Test Specimens. As-etched with $92HCl:5H_2SO_4:3HNO_3$. 300X.

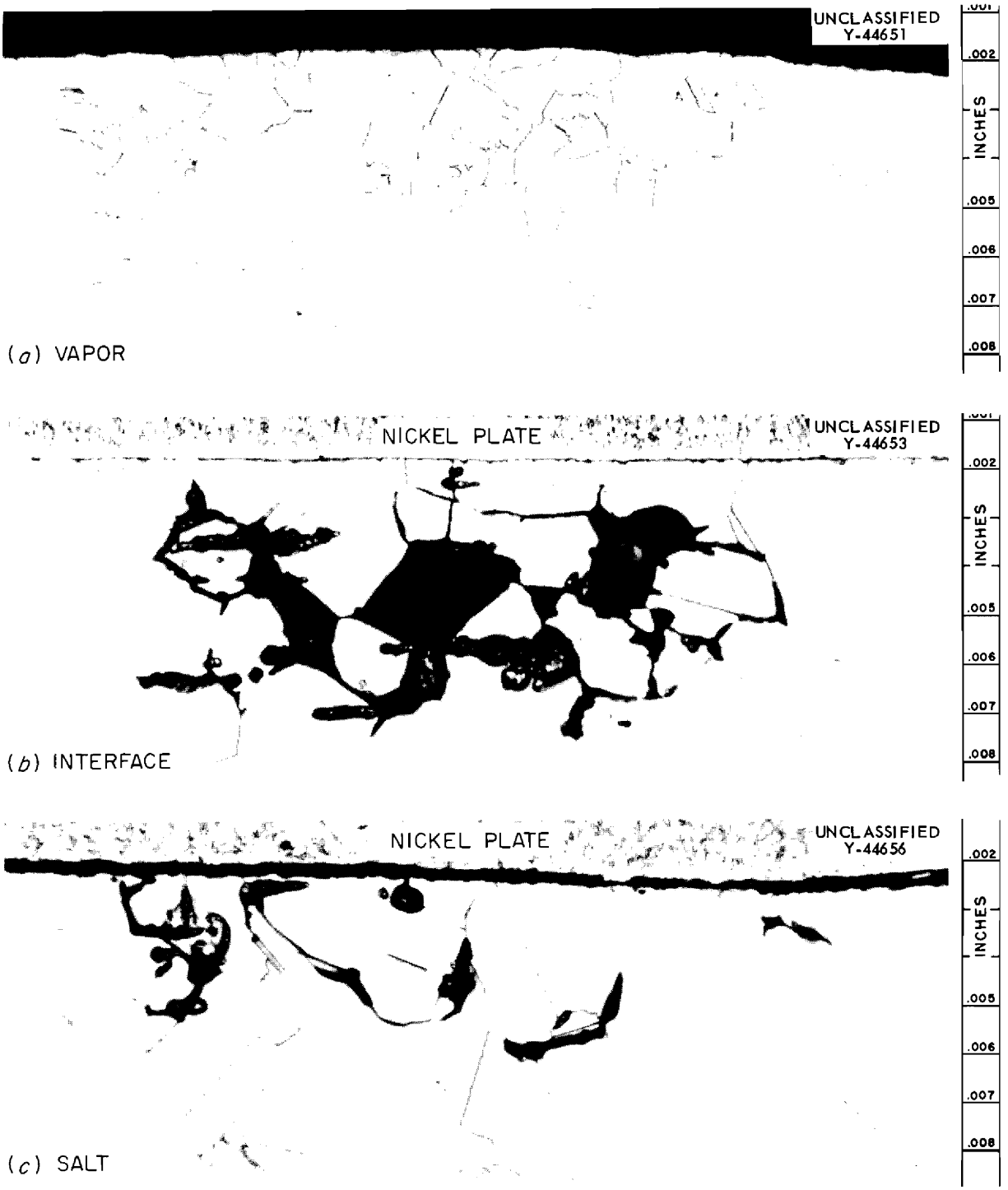

Fig. 22. Sections from L Nickel Specimen 55 from Group II Volatility Pilot Plant Fluorinator Test Specimens. As-etched with $92HCl:5H_2SO_4:3HNO_3$. 300X.

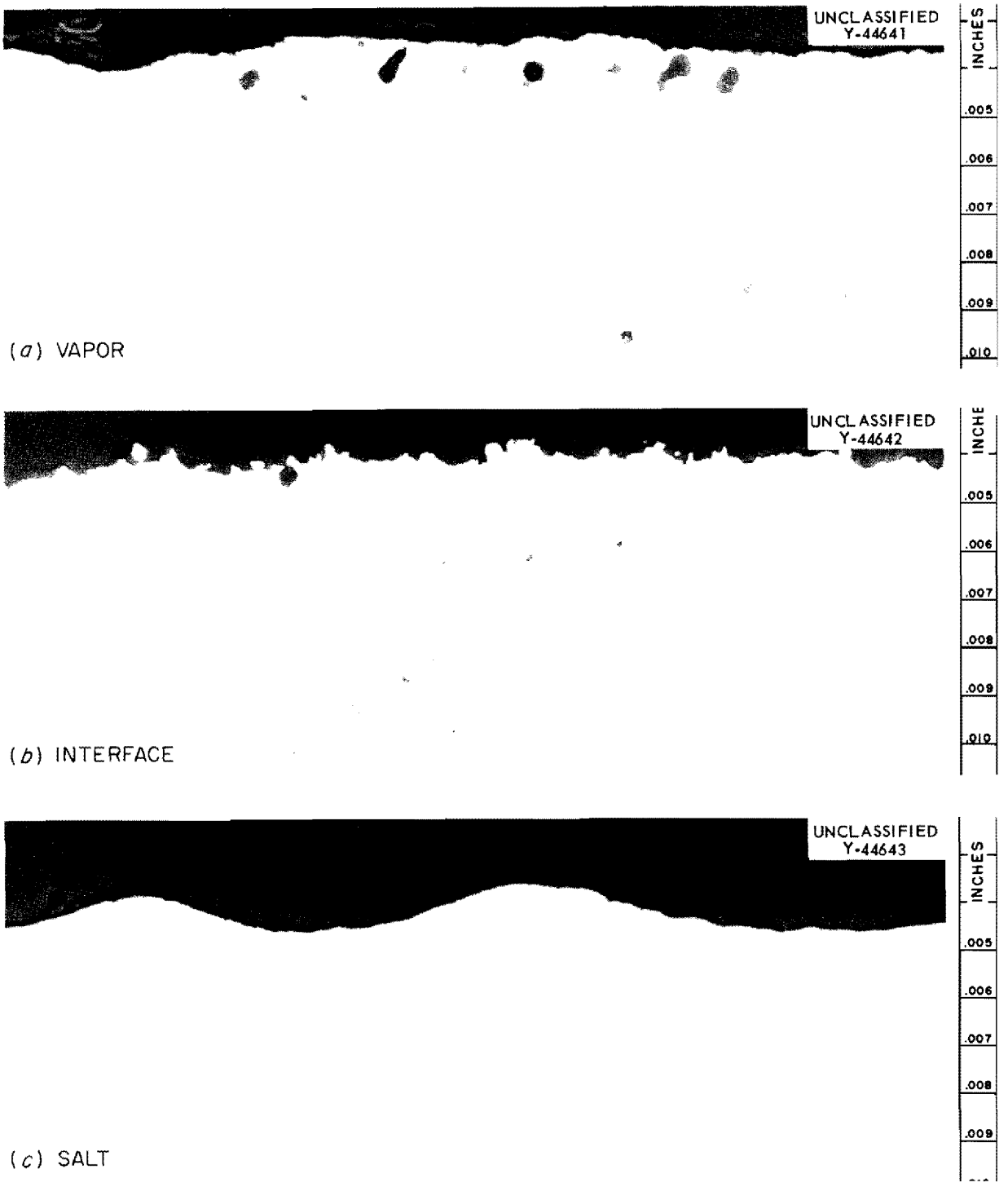

Fig. 23. Sections from INCO-61 Weld Deposits of Specimen 52 from Group II Volatility Pilot Plant Fluorinator Test Specimens. As-polished. 300X.

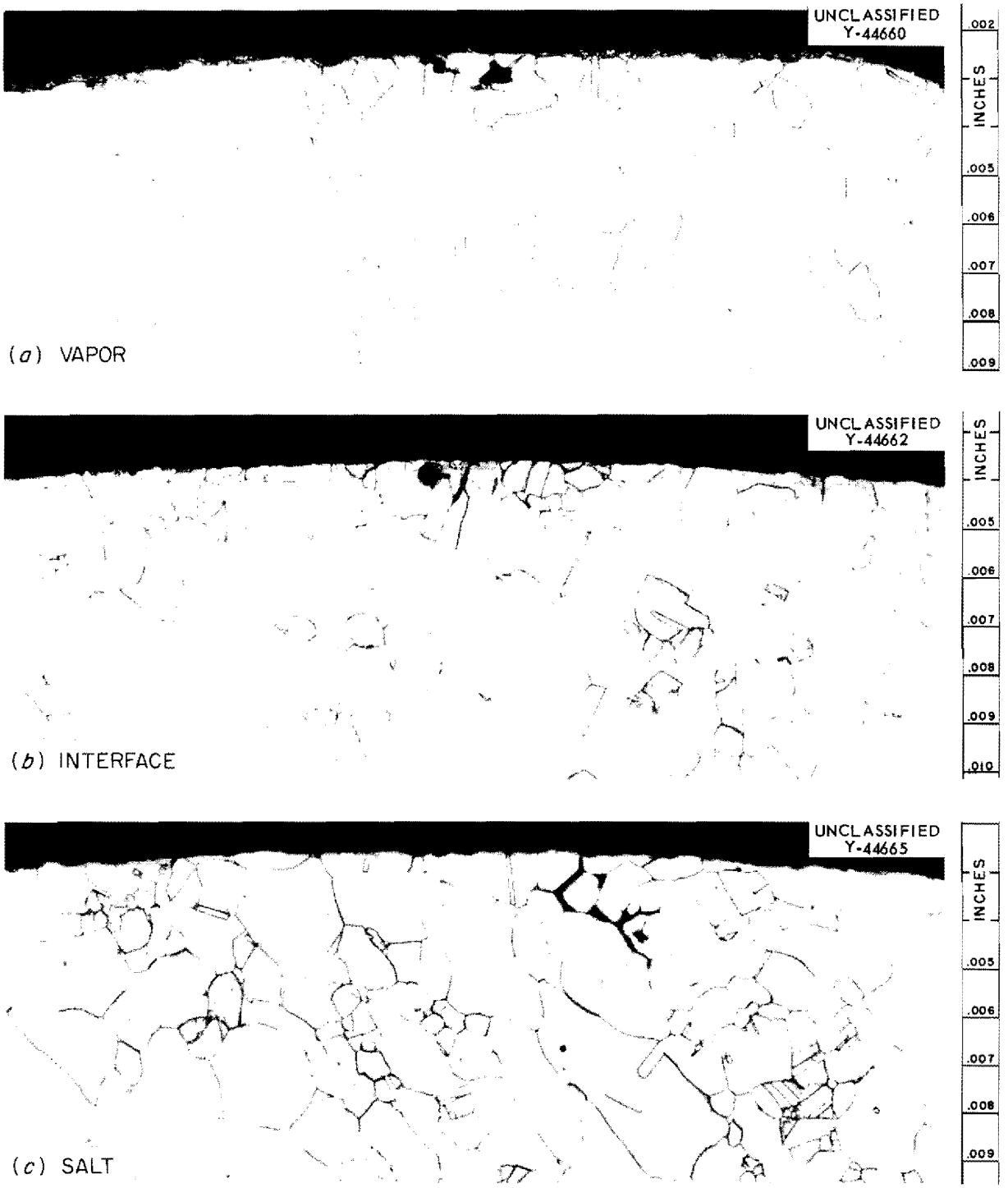

Fig. 24. Sections from 95 Ni–5 Co Specimen 17 from Group II Volatility Pilot Plant Fluorinator Test Specimens. As-etched with $92HCl:5H_2SO_4:3HNO_3$. 300X.

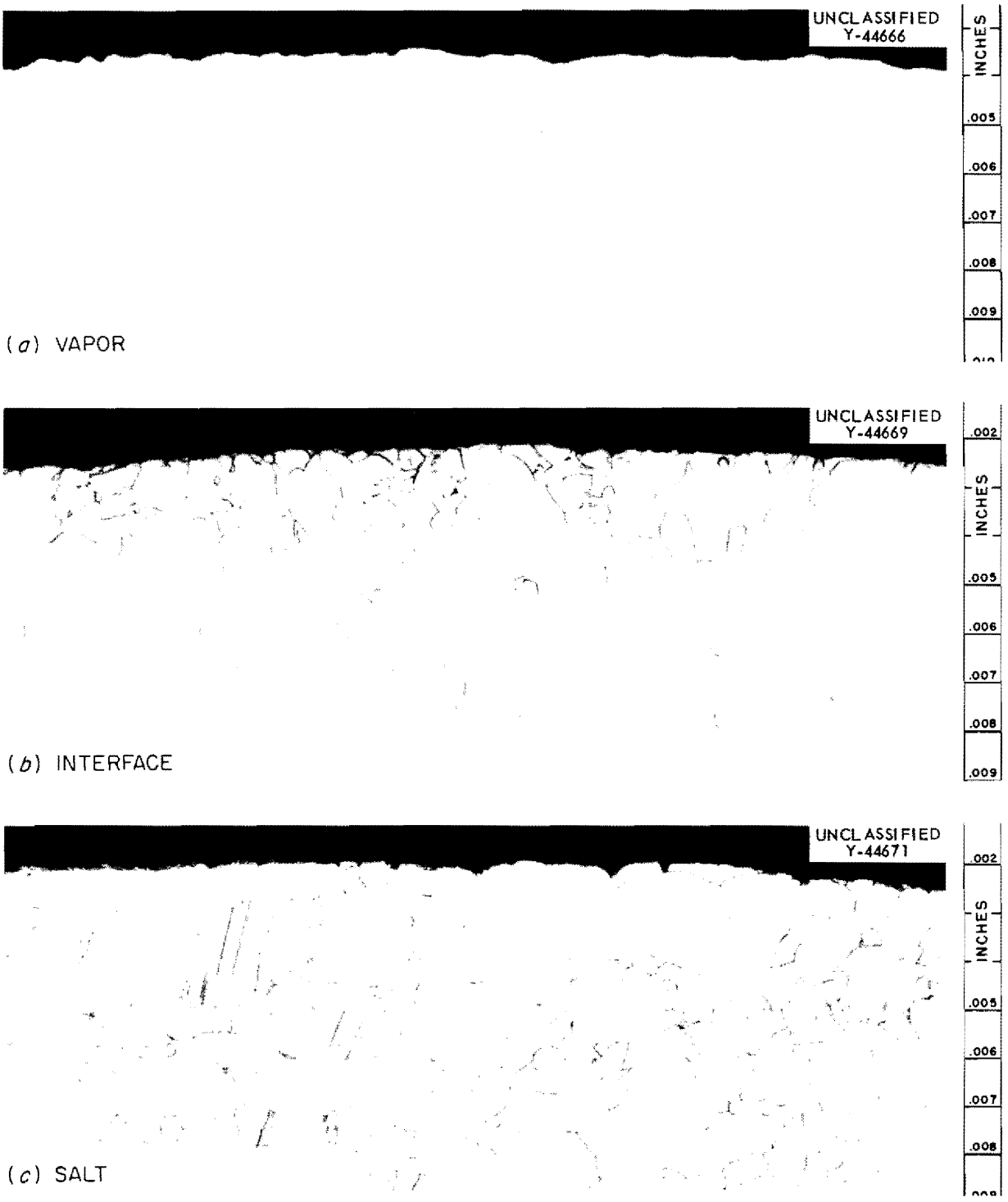

Fig. 25. Sections from 90 Ni–10 Co Specimen 21 from Group II Volatility Pilot Plant Fluorinator Test Specimens. Vapor section is as-polished. Interface and salt sections are as-etched with $92HCl:5H_2SO_4:3HNO_3$. 300X.

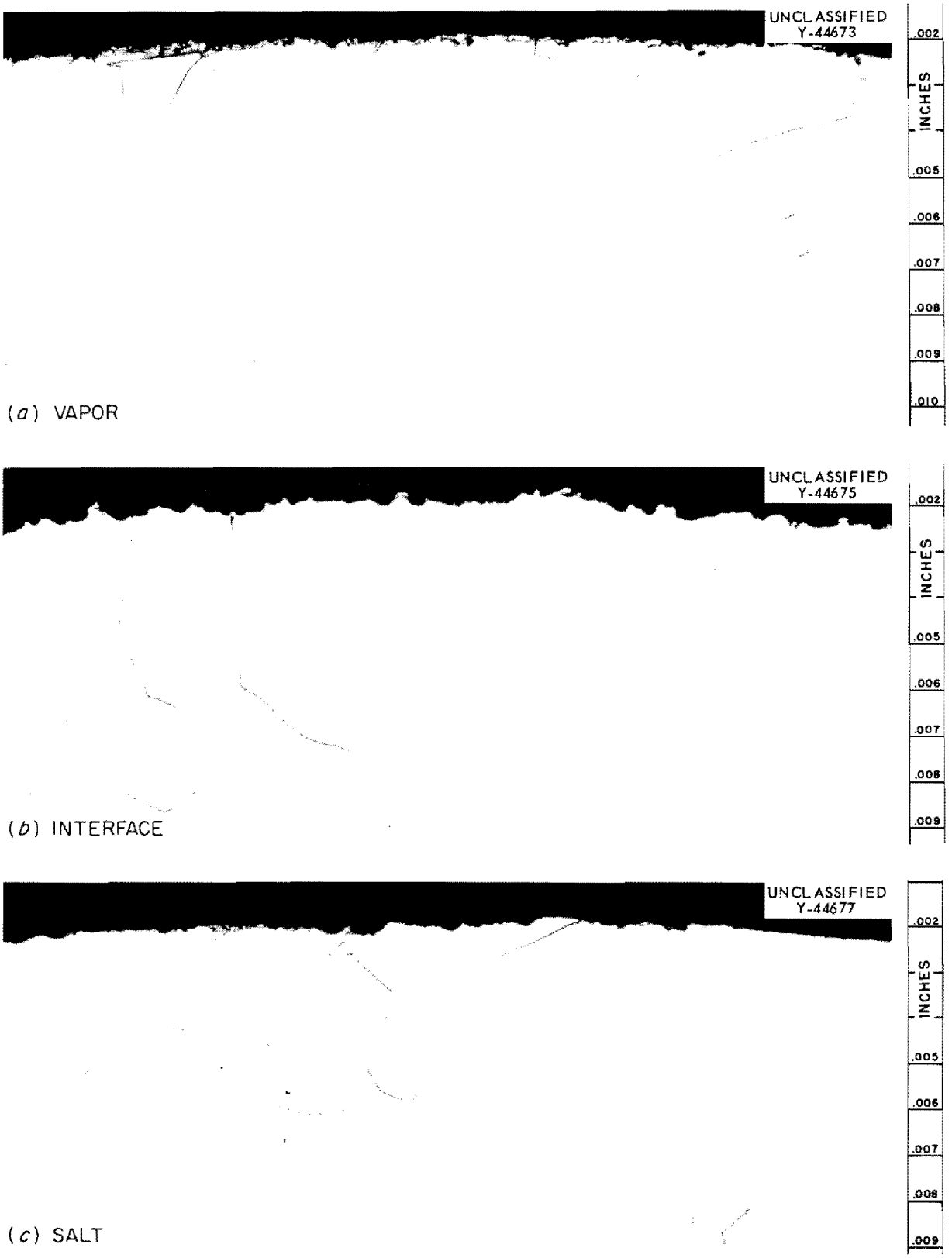

Fig. 26. Sections from 99 Ni–1 Al Specimen 1R from Group II Volatility Pilot Plant Fluorinator Test Specimens. As-etched with $92HCl:5H_2SO_4:3HNO_3$. 300X.

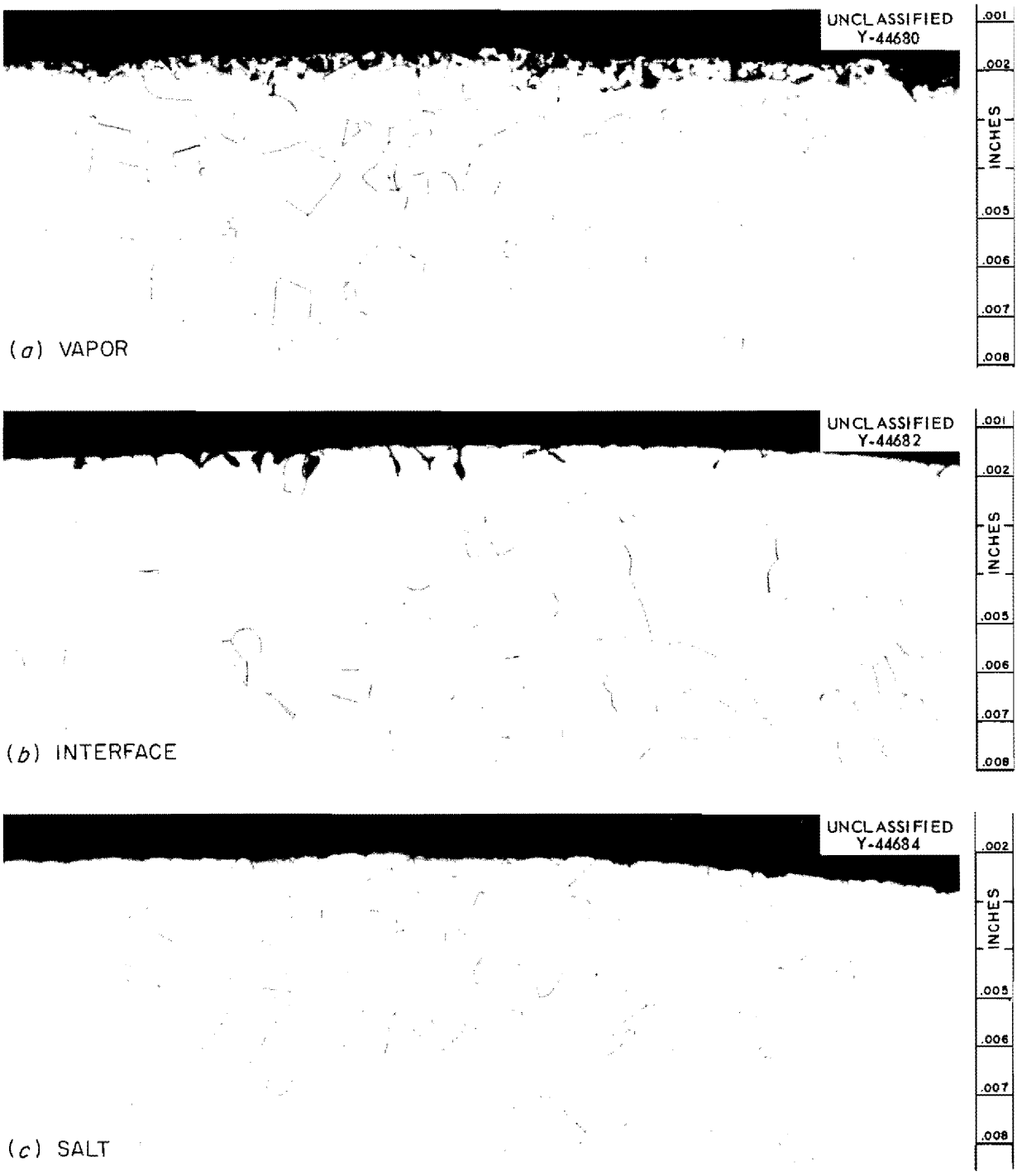

Fig. 27. Sections from 97 Ni–3 Al Specimen 5 from Group II Volatility Pilot Plant Fluorinator Test Specimens. As-etched with $92HCl:5H_2SO_4:3HNO_3$. 300X.

DISTRIBUTION

1. Biology Library
2–3. Central Research Library
4. Reactor Division Library
5. ORNL – Y-12 Technical Library Document Reference Section
6–20. Laboratory Records Department
21. Laboratory Records, ORNL R. C.
22. ORNL Patent Office
23. G. M. Adamson, Jr.
24–25. R. E. Blanco
26. J. C. Bresee
27. B. S. Borie
28. R. B. Briggs
29. K. B. Brown
30. W. H. Carr
31. G. I. Cathers
32. R. S. Crouse
33. F. L. Culler
34. J. E. Cunningham
35. J. H. DeVan
36. D. A. Douglas, Jr.
37. D. E. Ferguson
38. J. H Frye, Jr.
39. H. E. Goeller
40. C. E. Guthrie
41. R. J. Gray
42. W. R. Grimes
43. R. W. Horton
44–46. M. R. Hill
47. E. E. Hoffman
48. H. Inouye
49–51. T. M. Kegley, Jr.
52. E. Lamb
53. R. B. Lindauer
54–56. A. P. Litman
57. E. L. Long, Jr.
58. H. G. MacPherson
59. W. D. Manly
60. C. J. McHargue
61. R. P. Milford
62. E. C. Miller
63. E. C. Moncrief
64. A. R. Olsen
65. P. Patriarca
66. J. B. Ruch
67. S. H. Smiley
68. C. O. Smith
69. A. Taboada
70. W. C. Thurber
71. M. E. Whatley
72–86. Division of Technical Information Extension (DTIE)
87. Research and Development Division (ORO)
88. E. L. Anderson, AEC Washington
89. O. E. Dwyer, BNL
90. S. Lawroski, ANL
91. P. D. Miller, BMI
92. J. W. Nehls, ORO
93. C. M. Slanksky Phillips Petroleum Company, Idaho Falls